

Chiral perturbation theory and Bose-Einstein condensation in QCD

Jens O. Andersen,^{a,b} Martin Kjøllestad Johnsrud^{a,c} Qing Yu^d Hua Zhou^d

^a*Department of Physics, Faculty of Natural Sciences, NTNU, Norwegian University of Science and Technology, Høgskoleringen 5, N-7491 Trondheim, Norway*

^b*Niels Bohr International Academy, Blegdamsvej 17, DK-2100 Copenhagen, Denmark*

^c*Department of Living Matter Physics, Max Planck Institute of Dynamics and Self-Organization, Am Faßberg 17, DE-37077 Göttingen, Germany*

^d*Department of Physics, Chongqing University, Chongqing 401331, People's Republic of China*

E-mail: jens.andersen@ntnu.no, martin.johnsrud@ds.mpg.de,
yuq@swust.edu.cn, zhouhua@cqu.edu.cn

ABSTRACT: We present recent results in three-flavor chiral perturbation theory at finite isospin μ_I and strangeness μ_s chemical potentials at zero temperature. The phase diagram to $\mathcal{O}(p^2)$ in the μ_I - μ_S plane is mapped out with and without electromagnetic effects. The phase diagram consists of a vacuum phase and three Bose-condensed phases with condensates of π^\pm , K^\pm , and K^0/\bar{K}^0 , respectively. Including electromagnetic interactions, the Bose-condensed phases become Higgs phases via the Higgs mechanism. The tree-level spectrum for the mesons and gauge bosons is also derived. We calculate the pressure, energy density, isospin density, and speed of sound in the pion-condensed phase to $\mathcal{O}(p^4)$ for three-flavor χ PT. The results are compared with recent lattice simulations and the agreement is very good for isospin chemical potentials up to approximately 200 MeV. Moreover, by integrating out the s -quark, we show that the thermodynamic quantities can be mapped onto their two-flavor counterparts with renormalized parameters. We also consider the non-relativistic limit. It is shown that the energy density can be matched onto the classic result by Lee, Huang and Yang (LHY) for a dilute Bose, with an s -wave scattering length that includes radiative corrections. The breaking of the U(1) symmetry in the Bose-condensed phases gives rise to a Goldstone bosons, whose dispersion is linear for momenta $p \ll \mu_I$. In this regime, we use Son's prescription to construct an effective theory for the Goldstone field which is valid in this regime. It is shown that its damping rate is of order p^5 . This result is in agreement with Beliaev's for a dilute Bose gas.

Contents

1	Introduction	1
2	Chiral perturbation theory	4
3	Thermodynamic potential and thermodynamic quantities	9
4	Ground state and fluctuations at finite density	11
4.1	Form of the ground state	11
4.2	Fluctuations	14
5	Leading-order results	16
5.1	Quasiparticle masses	17
5.2	Connection to physical observables	20
5.3	Phase diagram	22
6	Thermodynamics at next-to-leading order	24
6.1	Thermodynamic potential and pressure	25
6.2	Large m_s -mass limit	27
6.3	Numerical results	28
7	Chiral limit of two-flavor χPT	31
8	Low-energy effective theory and phonon damping rate	33
9	Dilute Bose gas and the nonrelativistic limit of χPT	35
9.1	Dilute Bose gas	35
9.2	Nonrelativistic limit of χ PT	38
10	Summary and Outlook	39
A	Integrals in dimensional regularization	40

1 Introduction

The phase diagram of Quantum chromodynamics (QCD) has received a lot of attention in recent years due to its relevance for the early universe, heavy-ion collisions, and compact stars [1–3]. Conventionally, the phase diagram is shown in the plane of temperature T and baryon chemical potential μ_B . At finite μ_B , the sign problem of QCD poses a serious challenge. The fact that the fermion determinant is complex prohibits the use of importance sampling techniques in lattice simulations. By expanding the partition function in powers

of μ_B around zero, one can move away from the temperature axis into the μ_B - T plane, but obviously not too far. Part of the phase diagram has therefore been mapped out by low-energy models that share some of the properties of QCD, for example, the Nambu-Jona-Lasinio (NJL), quark-meson (QM) model, and their Polyakov-loop extended counterparts. Some aspects of the phase diagram are indicated in Fig. 1 in the μ_B - T plane showing for example a quarkyonic phase and a region where it is in a color superconducting phase.¹

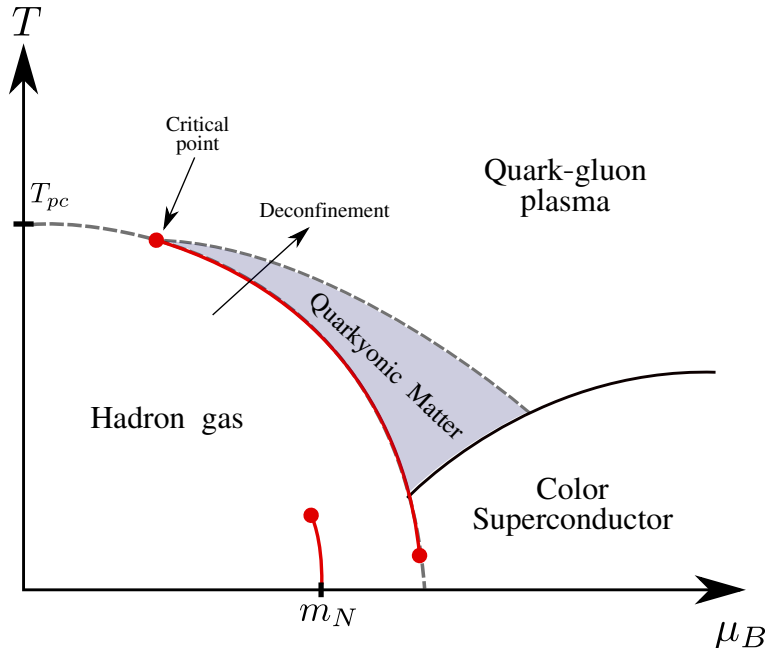


Figure 1. Schematic phase diagram of QCD in the μ_B - T plane. See main text for details.

Instead of using a common quark chemical potential $\mu_q = \frac{1}{3}\mu_B$ for the different flavors, one can introduce an independent chemical potential μ_f for $f = u, d, s$. They are expressed in terms of the baryon, isospin, and strangeness chemical potentials as $\mu_B = \frac{3}{2}(\mu_u + \mu_d)$, $\mu_I = (\mu_u - \mu_d)$, and $\mu_S = \frac{1}{2}(\mu_u + \mu_d - 2\mu_s)$.² In the special case $\mu_u = -\mu_d \neq 0$ and $\mu_s = 0$, only the isospin chemical potential μ_I is nonzero. From a theoretical point of view, QCD at zero baryon and strangeness chemical potentials but nonzero isospin chemical potential has the advantage that there is no sign problem: the fermion determinant is (manifestly) real and one can use standard importance sampling techniques to perform lattice simulations of the system. This opens up the possibility to compare predictions with low-energy effective theories such as chiral perturbation theory and models such as the NJL model and the quark-meson model. Chiral perturbation theory [4–7], first considered at finite μ_I in Ref. [8–10], is of particular interest since it gives model-independent predictions. Within its domain of validity, a comparison with lattice results can also be considered a check of the latter.

¹This part of the phase diagram is known to be very rich with a number of phases such as the color-flavor locked (CFL) phase, the two-flavor color superconducting (2SC) phase, and Larkin-Ovchinnikov-Fulde-Ferrel (LOFF) phases.

²This gives rise to a complicated three-dimensional phase diagram. In recent years, yet another aspect of QCD has been studied intensely, namely the behavior in the presence of a strong magnetic background.

The first simulations of two-flavor QCD at nonzero isospin chemical potential were performed twenty years ago using quenched lattice QCD [11, 12], which later was improved by including dynamical fermions [13] on relatively coarse lattices. Later, the simulations were extended to three-flavor QCD in the phase-quenched approximation [14, 15]. In recent years, high-precision lattice simulations have been carried out [16–22] and the phase diagram in the T – μ_I plane has been mapped out. Focusing on this part shown in Fig. 2, the solid black line is the phase boundary between the hadronic phase and the Bose-condensed phase, where the $U(1)_{I_3}$ symmetry is broken. The black dashed line is phase boundary between a confined and a deconfined phase. For large T and small μ_I this is the usual transition to a quark-gluon plasma.

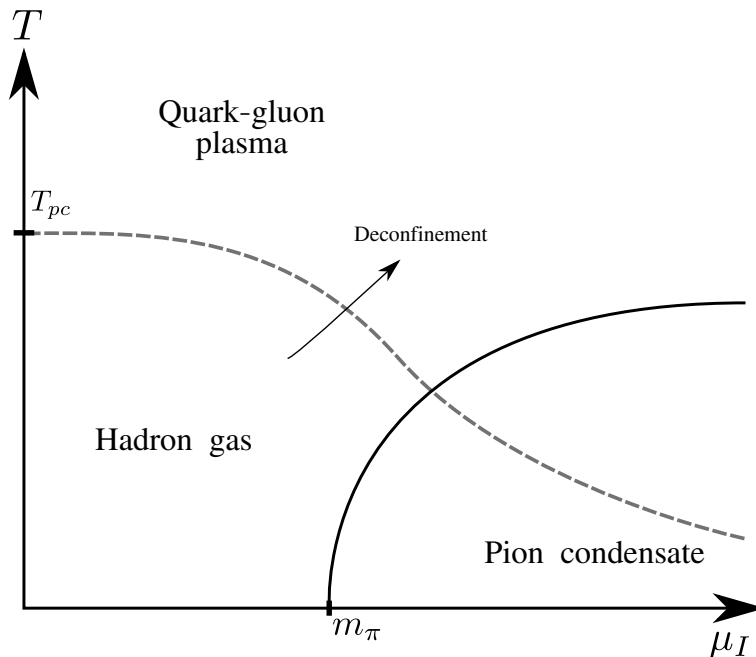


Figure 2. Phase diagram of QCD in the μ_I – T plane. See main text for details.

It has been shown both on the lattice and in χ PT that the transition at $T = 0$ from the vacuum phase to the pion-condensed phase takes place for a critical isospin chemical potential equal to the physical charged pion mass, $\mu_I^c = m_{\pi^\pm}$ and that the transition is second order. The transition remains second order at finite T along the solid black line. Moreover, the vacuum phase exhibits the so-called Silver-Blaze property, meaning that the thermodynamic properties at $T = 0$ are independent of the chemical potential μ_I all the way up to onset of Bose-Einstein condensation [23]. For asymptotically large values of μ_I , quarks rather than pions are the relevant degrees of freedom. Without interactions and low temperature, the system is described in terms of a Fermi surface. Turning on interactions, the Fermi surface is rendered unstable due to an attractive interaction channel provided by one-gluon exchange. The system then becomes a color superconductor, which is characterized by a BCS gap [8]. The transition from the BEC phase to the BCS phase is a crossover since the quantum numbers of the condensates are the same. This picture

is supported by lattice simulations [20, 21] and the crossover is indicated by a dashed line to the right in Fig. 2. Various aspects of dense QCD at finite isospin can be found in e.g. Refs. [24, 25] (χ PT), [26, 27] (NJL model), and [28–30] (QM model). Ref. [31] provides an application of χ PT in a magnetic field and a review meson condensation in QCD can be found in Ref. [32].

Electromagnetic interactions in chiral perturbation theory were first included at LO by Ecker et al. [33] and at NLO by Urech [34]. In Ref. [34], the NLO Lagrangian was derived and the leading corrections to the meson masses were computed, i.e. corrections to Dashen’s theorem [35]. Other early applications of χ PT to e.g. scattering of pions can be found in Ref. [36–38]. In the context of chiral perturbation theory, electromagnetic effects have not yet been included at finite isospin chemical potential. Since the spontaneously broken U(1) symmetry group corresponds to the local gauge group of electromagnetism, the Goldstone boson disappears from the physical spectrum and the photon becomes massive via the Higgs mechanism. The pion-condensed phase is then a superconductor and QCD is in a Higgs phase. The same remark applies to the phase of condensed charged kaons, but not to the phase of condensed neutral kaons. In this case, the phase is a superfluid. In this paper, we include the leading-order effects mapping out the phase diagram in the μ_I – μ_S plane. We also calculate the tree-level meson and gauge boson masses.

The plan of the paper is as follows. In sections 1-4, we briefly review chiral perturbation theory and how one does systematic calculations at finite chemical potentials. In sections 5-6, we apply χ PT to dense QCD at finite isospin and strangeness chemical potential. The quasiparticle masses and the phase diagram are calculated to leading order in the low-energy expansion. The thermodynamic potential and various thermodynamic quantities are derived to next-to-leading order and the results are compared with lattice simulations. In section 7, we discuss the chiral limit and in section. 8, we derive the low-energy effective theory for the massless Goldstone boson in the pion-condensed phase. We also consider the nonrelativistic limit of the system and show that it behaves as a dilute Bose gas close to the phase transition. Some calculational details and formulas can be found in an Appendix.

2 Chiral perturbation theory

In this section, we briefly discuss the construction of the low-energy chiral Lagrangian using the coset construction. This has been done in detail many times in the literature. Some of the original references are [39, 40], while more recent introduction to effective field theory can be found in Refs. [41, 42]. The QCD Lagrangian with massless quarks has an $SU(N)_L \times SU(N)_R$ global symmetry which in the vacuum is broken down to $SU(N)_V$ by the quark condensate. The vacuum manifold is then $SU(N)_L \times SU(N)_R / SU(N)_V \sim SU(N)$. The vacuum manifold of the effective low-energy theory can be parametrized as

$$\Sigma = \Sigma_0 e^{i\phi_a X_a / f}, \quad (2.1)$$

where Σ_0 is the vacuum state, X_a are the broken symmetry generators, ϕ_a are the Goldstone fields, and f is the (bare) pion decay constant. For two flavors, the broken generators are the Pauli matrices τ_a and in the three-flavor case, the broken generators are the Gell-Mann

matrices λ_a . They are normalized as $\langle \tau_a \tau_b \rangle = \langle \lambda_a \lambda_b \rangle = 2\delta_{ab}$, where $\langle A \rangle$ denotes the trace of the matrix A . Under $SU(N)_L \times SU(N)_R$ transformations L and R , Σ transforms as

$$\Sigma \rightarrow \Sigma' = R\Sigma L^\dagger. \quad (2.2)$$

The fundamental object or building block in the coset construction is the so-called Maurer-Cartan form

$$d_\mu = i\Sigma^\dagger \partial_\mu \Sigma, \quad (2.3)$$

which is an element of the $\mathfrak{su}(N)$ algebra. One constructs the invariant terms in the Lagrangian by taking traces of products of Eq. (2.3). Each factor of d_μ counts as one power of momentum via the derivative of Σ . The leading term $\langle d_\mu \rangle$ clearly vanishes since the generators of $SU(N)$ are traceless. The next term is the trace of a product of two d_μ 's with indices contracted so it is Lorentz invariant. At leading order in the low-energy expansion, the Lagrangian is therefore

$$\mathcal{L}_2 = \frac{1}{4} f^2 \langle \partial_\mu \Sigma^\dagger \partial^\mu \Sigma \rangle, \quad (2.4)$$

The bare pion constant f cannot be determined by symmetry considerations alone. At tree-level, f is identified with the pion-decay constant $f = f_\pi$, however, this relation receives corrections once loops are taken into account.

In real-world QCD, the current quark masses are nonzero. This explicit symmetry breaking in the QCD Lagrangian gives rise to symmetry breaking terms in the chiral Lagrangian. Similarly, electroweak interactions also break chiral symmetry. For example, we cannot rotate a u quark into a d quark since they have different electric charges. Finally, for each intact global symmetry, we may introduce an independent chemical potential μ_i in the QCD Lagrangian. However, this can be done simultaneously for μ_i and μ_j only if the corresponding charges commute. In QCD, we can then introduce an independent chemical potential μ_f for each quark flavor f . In order to incorporate these effects in the chiral Lagrangian, it is convenient to couple the QCD Lagrangian to external fields v_μ , a_μ , s , and p as [5, 34]

$$\mathcal{L}_{\text{QCD}} = -\frac{1}{2g^2} \langle G_{\mu\nu} G^{\mu\nu} \rangle + i\bar{q}\gamma^\mu D_\mu q + \bar{q}\gamma^\mu (v_\mu + \gamma^5 a_\mu) q - \bar{q}(s - i\gamma^5 p)q. \quad (2.5)$$

Here, $G_{\mu\nu}$ is the field-strength tensor of the strong force and $D_\mu = \partial_\mu - igT_a \mathcal{A}_\mu^a$ is the corresponding covariant derivatives where T_a are the $SU(3)$ generators and \mathcal{A}_μ^a is the gluon field. The external fields are then evaluated at nonvanishing values corresponding to the symmetry-breaking terms. These are

$$s = M = \text{diag}(m_u, m_d, m_s), \quad (2.6)$$

$$p = \lambda_a j, \quad (2.7)$$

$$l_\mu = v_\mu - a_\mu = \delta_{0\mu} \text{diag}(\mu_u, \mu_d, \mu_s) + Q_L A_\mu, \quad (2.8)$$

$$r_\mu = v_\mu + a_\mu = \delta_{0\mu} \text{diag}(\mu_u, \mu_d, \mu_s) + Q_R A_\mu, \quad (2.9)$$

with $Q_R = Q_L = e \text{diag}(\frac{2}{3}, -\frac{1}{3}, -\frac{1}{3})$ is the quark charge matrix and μ_f is the quark chemical potential for flavor f ($f = u, d, s$), and $e > 0$ is the fundamental electric charge. The source s accounts for the quark masses, while A_μ is the electromagnetic field, and μ_f accounts for finite density. The pseudoscalar source $p = \lambda_a j$ is needed if we want to calculate a Bose condensate. We choose $a = 2, 5$, or 7 depending on the condensate of interest, π^\pm , K^\pm or K^0/\bar{K}^0 . Instead of using the quark chemical potentials μ_f , we can express the left-handed and right-handed fields in terms of the baryon, isospin, and strangeness chemical potentials μ_B , μ_I and μ_S using

$$\text{diag}(\mu_u, \mu_d, \mu_s) = \frac{1}{3}(\mu_B - \mu_S)\mathbb{1} + \frac{1}{2}\mu_I\lambda_3 + \frac{1}{\sqrt{3}}\mu_S\lambda_8, \quad (2.10)$$

with

$$\mu_B = \frac{3}{2}(\mu_u + \mu_d), \quad \mu_I = \mu_u - \mu_d, \quad \mu_S = \frac{1}{2}(\mu_u + \mu_d - 2\mu_s). \quad (2.11)$$

The $SU(3)_L \times SU(3)_R$ invariance in QCD can be made local provided the left-handed and right-handed fields q_L and q_R , and the external fields transform as

$$q_L \rightarrow Lq_L, \quad q_R \rightarrow Rq_R, \quad (s + ip) \rightarrow R(s + ip)L^\dagger, \quad (2.12)$$

$$l_\mu \rightarrow Ll_\mu L^\dagger + iL\partial_\mu L^\dagger, \quad r_\mu \rightarrow Rr_\mu R^\dagger + iR\partial_\mu R^\dagger, \quad Q_L \rightarrow LQ_L L^\dagger, \quad (2.13)$$

$$Q_R \rightarrow RQ_R R^\dagger. \quad (2.14)$$

In the effective theory, the local invariance is implemented by replacing the partial derivative by a covariant derivative as

$$\partial_\mu \Sigma \rightarrow \nabla_\mu \Sigma = \partial_\mu \Sigma - ir_\mu \Sigma + i\Sigma l_\mu, \quad (2.15)$$

$$\partial_\mu \Sigma^\dagger \rightarrow \nabla_\mu \Sigma^\dagger = \partial_\mu \Sigma^\dagger + i\Sigma^\dagger r_\mu - il_\mu \Sigma^\dagger. \quad (2.16)$$

One can now use the building blocks Σ , Σ^\dagger , $\nabla_\mu \Sigma$, $\nabla_\mu \Sigma^\dagger$, and $s \pm ip$ to build invariant terms. Of course, the external fields do not transform according to Eqs. (2.12)–(2.14), once they take the constant values, the symmetries are explicitly broken. However, by construction the symmetries in the effective theory are broken in the same way as in QCD. Specifically, the introduction of the quark chemical potentials breaks the $SU(3)_V$ down to $U(1) \times U(1)$, as can be seen by Eq. (2.10). More generally, one can introduce as many independent chemical potentials as there are commuting charges [43, 44], which is the dimension of the Cartan subalgebra. For the group $SU(3)$ the subalgebra consists of the two matrices λ_3 and λ_8 . There are other choices that may be convenient when discussing kaon condensation in QCD. Eq. (2.10) can be written as

$$\text{diag}(\mu_u, \mu_d, \mu_s) = \frac{1}{3}(\mu_B - \mu_S)\mathbb{1} + \frac{1}{2}\mu_{K^\pm}\lambda_Q + \frac{1}{2}\mu_{K^0}\lambda_K, \quad (2.17)$$

where $\lambda_Q = \lambda_3 + \frac{1}{\sqrt{3}}\lambda_8$ and $\lambda_K = -\lambda_3 + \frac{1}{\sqrt{3}}\lambda_8$ and the corresponding chemical potentials are $\mu_{K^\pm} = \frac{1}{2}\mu_I + \mu_S$ and $\mu_{K^0} = -\frac{1}{2}\mu_I + \mu_S$, respectively. These are the combinations of μ_I and μ_S that correspond to the quark content of the charged and neutral kaons. When the absolute values exceed the relevant kaon mass, it forms a Bose condensate, as we shall see below.

The organization of the effective Lagrangian in a systematic low-energy expansion requires a consistent power-counting scheme. The original scheme of Gasser and Leutwyler [5, 6], which does not take into account electromagnetic effects, is such that a derivative counts as $\mathcal{O}(p)$ as does one quark mass. The leading derivative term is already given in Eq. (2.4), but there is another term proportional to $\langle \Sigma^\dagger \chi + \chi^\dagger \Sigma \rangle$, where $\chi = 2B_0(s + ip)$ and B_0 is a constant related to the chiral quark condensate. The leading-order Lagrangian is then

$$\mathcal{L}_2 = \frac{1}{4}f^2 \langle \nabla_\mu \Sigma^\dagger \nabla^\mu \Sigma \rangle + \frac{1}{4}f^2 \langle \Sigma^\dagger \chi + \chi^\dagger \Sigma \rangle, \quad (2.18)$$

where the covariant derivatives are given by the right-hand side of Eqs. (2.15)–(2.16) but with $l_\mu = r_\mu = \delta_{0\mu} \text{diag}(\mu_u, \mu_d, \mu_s)$. If we include electromagnetic terms, we need additional counting rules, which were provided by Urech [34]. Since v_μ is of order p , the term QA_μ has the same dimension. The charge e and the field A_μ are assigned to be of order p and order one, respectively. This rule does not alter the standard chiral counting. In addition to including A_μ in the covariant derivative above, there is a new term $\langle Q_L \Sigma Q_R \Sigma^\dagger \rangle$ such that the leading-order Lagrangian is

$$\begin{aligned} \mathcal{L}_2 = & -\frac{1}{4}F_{\mu\nu}F^{\mu\nu} + \frac{1}{4}f^2 \langle \nabla_\mu \Sigma \nabla^\mu \Sigma \rangle + \frac{1}{4}f^2 \langle \Sigma^\dagger \chi + \chi^\dagger \Sigma \rangle + C \langle Q \Sigma Q \Sigma^\dagger \rangle \\ & + \mathcal{L}_{\text{gf}} + \mathcal{L}_{\text{ghost}} - eA_\mu J_{\text{back}}^\mu, \end{aligned} \quad (2.19)$$

where the first term is the kinetic term for photons, C is a coupling constant and the the gauge-fixing Lagrangian in general R_ξ gauge is

$$\mathcal{L}_{\text{gf}} = \frac{1}{2\xi} (\partial_\mu A^\mu + \xi e f \sin \alpha \phi_1)^2, \quad (2.20)$$

where ξ is a gauge parameter in the class of covariant gauges. The counterterms at next-to-leading order, which we have not listed, are known in Feynman gauge only, $\xi = 1$, [34]. Denoting the ghost field by c , the ghost Lagrangian is

$$\mathcal{L}_{\text{ghost}} = \partial_\mu \bar{c} \partial^\mu c - \xi e^2 f^2 \sin^2 \alpha \bar{c} c - \xi e^2 f \sin \alpha \phi_1 \bar{c} c. \quad (2.21)$$

Finally, the last term is the coupling of the gauge field to background charges and currents J_{back}^μ . This term is necessary to ensure overall electric neutrality [43]. We will not need it in the remainder of the paper.

At next-to-leading order, there are many more terms in the chiral Lagrangian. For general $\text{SU}(N)$, there are 13 independent terms in addition to contact terms (contact terms are terms that depend only on the external fields). For two flavors, there are 10 terms and an additional 14 terms if we include electromagnetism [5, 34]. For three flavors the number of operators are 12 and 17, respectively [6, 34]. The reduction in the number of terms for $N_f = 2$ and $N_f = 3$ is due to the fact that not all terms in the $\text{SU}(N_f)$ case are linearly independent. Not all of the terms in the $N_f = 2$ and $N_f = 3$ case are relevant to the present work. Ignoring electromagnetic effects, the operators we need in the three-flavor case are

$$\begin{aligned} \mathcal{L}_4 = & L_1 \langle \nabla_\mu \Sigma^\dagger \nabla^\mu \Sigma \rangle^2 + L_2 \langle \nabla_\mu \Sigma^\dagger \nabla_\nu \Sigma \rangle \langle \nabla^\mu \Sigma^\dagger \nabla^\nu \Sigma \rangle + L_3 \langle (\nabla_\mu \Sigma^\dagger \nabla^\mu \Sigma) (\nabla_\nu \Sigma^\dagger \nabla^\nu \Sigma) \rangle \\ & + L_4 \langle \nabla_\mu \Sigma^\dagger \nabla^\mu \Sigma \rangle \langle \chi^\dagger \Sigma + \chi \Sigma^\dagger \rangle + L_5 \langle (\nabla_\mu \Sigma^\dagger \nabla^\mu \Sigma) (\chi^\dagger \Sigma + \chi \Sigma^\dagger) \rangle \\ & + L_6 \langle \chi^\dagger \Sigma + \chi \Sigma^\dagger \rangle^2 + L_7 \langle \chi \Sigma - \chi \Sigma^\dagger \rangle^2 + L_8 \langle \chi^\dagger \Sigma \chi^\dagger \Sigma + \chi \Sigma^\dagger \chi \Sigma^\dagger \rangle + H_2 \langle \chi \chi^\dagger \rangle. \end{aligned} \quad (2.22)$$

The parameters L_1 – L_8 are low-energy constants, while the parameter H_2 is referred to as a high-energy constant. The relation between the bare and renormalized parameters is

$$L_i = L_i^r - \frac{\Lambda^{-2\epsilon}\Gamma_i}{2(4\pi)^2} \left[\frac{1}{\epsilon} + 1 \right], \quad H_i = H_i^r - \frac{\Lambda^{-2\epsilon}\Delta_i}{2(4\pi)^2} \left[\frac{1}{\epsilon} + 1 \right]. \quad (2.23)$$

The constants are Γ_i and Δ_i assume the following values [6]

$$\Gamma_1 = \frac{3}{32}, \quad \Gamma_2 = \frac{3}{16}, \quad \Gamma_3 = 0, \quad \Gamma_4 = \frac{1}{8}, \quad \Gamma_5 = \frac{3}{8}, \quad (2.24)$$

$$\Gamma_6 = \frac{11}{144}, \quad \Gamma_7 = 0, \quad \Gamma_8 = \frac{5}{48}, \quad \Delta_2 = \frac{5}{24}. \quad (2.25)$$

The renormalized couplings L_i^r and H_i^r are scale-dependent and run to ensure the scale independence of observables in χ PT. Since the bare couplings are independent of Λ , differentiation of Eqs. (2.23) with respect to the scale yields

$$\Lambda \frac{dL_i^r}{d\Lambda} = -\frac{\Lambda^{-2\epsilon}\Gamma_i}{(4\pi)^2} [1 + \epsilon], \quad \Lambda \frac{dH_i^r}{d\Lambda} = -\frac{\Lambda^{-2\epsilon}\Delta_i}{(4\pi)^2} [1 + \epsilon]. \quad (2.26)$$

We note that $\Gamma_3 = \Gamma_7 = 0$, which implies that L_3^r and L_7^r do not run, we therefore write $L_3 = L_3^r$ and $L_7 = L_7^r$. The solutions to these equations are

$$L_i^r(\Lambda) = L_i^r(\Lambda_0) + \frac{\Gamma_i}{2(4\pi)^2} (\Lambda^{-2\epsilon} - \Lambda_0^{-2\epsilon}) \left[\frac{1}{\epsilon} + 1 \right], \quad (2.27)$$

$$H_i^r(\Lambda) = H_i^r(\Lambda_0) + \frac{\Delta_i}{2(4\pi)^2} (\Lambda^{-2\epsilon} - \Lambda_0^{-2\epsilon}) \left[\frac{1}{\epsilon} + 1 \right], \quad (2.28)$$

where Λ_0 is a reference scale. In the limit $\epsilon \rightarrow 0$, the solutions reduce to

$$L_i^r(\Lambda) = L_i^r(\Lambda_0) - \frac{\Gamma_i}{2(4\pi)^2} \log \frac{\Lambda^2}{\Lambda_0^2}, \quad H_i^r(\Lambda) = H_i^r(\Lambda_0) - \frac{\Delta_i}{2(4\pi)^2} \log \frac{\Lambda^2}{\Lambda_0^2}. \quad (2.29)$$

In the two-flavor case, the relevant terms in NLO Lagrangian are ³

$$\begin{aligned} \mathcal{L}_4 = & \frac{1}{4} l_1 \langle \nabla_\mu \Sigma^\dagger \nabla^\mu \Sigma \rangle^2 + \frac{1}{4} l_2 \langle \nabla_\mu \Sigma^\dagger \nabla_\nu \Sigma \rangle \langle \nabla^\mu \Sigma^\dagger \nabla^\nu \Sigma \rangle + \frac{1}{16} (l_3 + l_4) \langle \chi^\dagger \Sigma + \Sigma^\dagger \chi \rangle^2 \\ & + \frac{1}{8} l_4 \langle \nabla_\mu \Sigma^\dagger \nabla^\mu \Sigma \rangle \langle \chi^\dagger \Sigma + \Sigma^\dagger \chi \rangle - \frac{1}{16} l_7 \langle \chi^\dagger \Sigma - \Sigma^\dagger \chi \rangle^2 + \frac{1}{2} h_1 \langle \chi^\dagger \chi \rangle, \end{aligned} \quad (2.30)$$

where l_1 – l_4 , l_7 and h_1 are bare coupling constants.⁴ The relations between the bare couplings and their renormalized counterparts are

$$l_i = l_i^r - \frac{\gamma_i \Lambda^{-2\epsilon}}{2(4\pi)^2} \left[\frac{1}{\epsilon} + 1 \right], \quad h_i = h_i^r - \frac{\delta_i \Lambda^{-2\epsilon}}{2(4\pi)^2} \left[\frac{1}{\epsilon} + 1 \right], \quad (2.31)$$

where γ_i and δ_i are pure numbers

$$\gamma_1 = \frac{1}{3}, \quad \gamma_2 = \frac{2}{3}, \quad \gamma_3 = -\frac{1}{2}, \quad \gamma_4 = 2, \quad \delta_1 = 0. \quad (2.32)$$

³The expression in [5] is written using $O(4)$ vector notation, instead of the more common $SU(2)_L \times SU(2)_R$ matrix notation employed in this text. This leads to some additional numerical factors. The conversion is explained in Appendix D of [45].

⁴ h_1 in this text corresponds to $h_1 - l_4$ in [5] due to rewriting of terms [48].

The parameters satisfy renormalization group equations similar to Eqs. (2.26) with solutions that specify their running. For $\epsilon = 0$, the solution is

$$l_i^r(\Lambda) = \frac{\gamma_i}{2(4\pi)^2} \left[\bar{l}_i + \log \frac{m_{\pi,0}^2}{\Lambda^2} \right], \quad (2.33)$$

where \bar{l}_i are constants. Up to a prefactor these constants equal l_i^r evaluated at the scale of the (bare) pion mass. In the two-flavor case, we will be computing the NNLO pressure in chiral limit in section 7. In this limit, $m_{\pi,0} \rightarrow 0$, so we will use the running coupling $l_i^r(\Lambda)$ instead.

At $\mathcal{O}(p^6)$, the Lagrangian contains a larger number of terms, 57 for SU(2) and 94 for SU(3) [46, 47]. Most of them vanish in the chiral limit and for two flavors, the set of operators reduces to

$$\begin{aligned} \mathcal{L}_6 = & C_{24} \langle (\nabla_\mu \Sigma^\dagger \nabla^\mu \Sigma)^3 \rangle + C_{25} \langle \nabla_\rho \Sigma^\dagger \nabla^\rho \Sigma \nabla_\mu \Sigma^\dagger \nabla_\nu \Sigma \nabla^\mu \Sigma^\dagger \nabla^\nu \Sigma \rangle \\ & + C_{26} \langle \nabla_\mu \Sigma^\dagger \nabla_\nu \Sigma \nabla_\rho \Sigma^\dagger \nabla^\mu \Sigma \nabla^\nu \Sigma^\dagger \nabla^\rho \Sigma \rangle, \end{aligned} \quad (2.34)$$

where C_{24} – C_{26} are couplings. The relation between the bare couplings C_i and renormalized couplings C_i^r is

$$C_i = \frac{C_i^r \Lambda^{-4\epsilon}}{f^2} - \frac{\gamma_i^{(2)} \Lambda^{-4\epsilon}}{4(4\pi)^4 f^2} \left[\frac{1}{\epsilon} + 1 \right]^2 + \frac{(\gamma_i^{(1)} \Lambda^{-2\epsilon} + \gamma_i^{(L)}) \Lambda^{-2\epsilon}}{2(4\pi)^2 f^2} \left[\frac{1}{\epsilon} + 1 \right], \quad (2.35)$$

where the relevant coefficients are

$$\gamma_{24}^{(1)} = -\frac{1}{(4\pi)^2} \frac{9}{32}, \quad \gamma_{25}^{(1)} = -\frac{1}{(4\pi)^2} \frac{67}{432}, \quad \gamma_{26}^{(1)} = \frac{1}{(4\pi)^2} \frac{449}{864}, \quad (2.36)$$

$$\gamma_{24}^{(2)} = -\frac{137}{72}, \quad \gamma_{25}^{(2)} = \frac{5}{36}, \quad \gamma_{26}^{(2)} = \frac{55}{72}, \quad (2.37)$$

$$\gamma_{24}^{(L)} = -2l_1^r - \frac{16}{3}l_2^r - \frac{5}{4}l_6^r, \quad \gamma_{25}^{(L)} = 2l_1^r - \frac{1}{3}l_2^r + \frac{1}{2}l_6^r, \quad \gamma_{26}^{(L)} = \frac{8}{3}l_2^r + \frac{3}{4}l_6^r. \quad (2.38)$$

In section 7, we need the combination $C = C_{24} + C_{25} + C_{26}$. The renormalized coupling $C^r = C_{24}^r + C_{25}^r + C_{26}^r$ satisfies the renormalization group equation

$$\Lambda \frac{dC^r}{d\Lambda} = \frac{1}{6(4\pi)^4} - \frac{3l_2^r}{(4\pi)^2}. \quad (2.39)$$

which again follows from the scale independence of the bare coupling C .

3 Thermodynamic potential and thermodynamic quantities

The thermodynamic potential Ω is the object we are interested in since we can calculate quantities such as the pressure, charge densities, and energy density from it. The thermodynamic potential typically depends on particle masses m_i , one or more chemical potentials μ_i as well as other parameters that we denote by α . We have seen that for zero baryon chemical potential, we have two independent chemical potentials e.g. μ_I and μ_S . However,

the phases we discuss in this paper are always described in terms of a single chemical potential, either μ_I or $\pm\frac{1}{2}\mu_I + \mu_S$. Similarly, the thermodynamic potential depends on a single additional parameter α , which in QCD can be identified with the rotation angle of the vacuum (see next section) and is nonzero in the Bose-condensed phases. When we discuss the weakly interacting Bose gas, the parameter is denoted by v , which is the condensate density. In the following we therefore write $\Omega(\mu, \alpha)$.

The thermodynamic potential can be systematically expanded in powers of p/f in χ PT and in powers of the so-called (dimensionless) gas parameter $\sqrt{na^3}$ in the case of the dilute Bose gas. Thus we write

$$\Omega(\mu, \alpha) = \Omega_0(\mu, \alpha) + \Omega_1(\mu, \alpha) + \dots, \quad (3.1)$$

where the subscript n denotes the n th-order contribution in the series. The value of α that extremizes the thermodynamic potential for a given μ is found by solving

$$\frac{\partial\Omega(\mu, \alpha)}{\partial\alpha} = 0, \quad (3.2)$$

and is denoted by α^* . The pressure \mathcal{P} is equal to minus the thermodynamic potential evaluated $\alpha = \alpha^*$, i.e.

$$\mathcal{P}(\mu) = -\Omega(\mu, \alpha^*). \quad (3.3)$$

The charge density n_Q associated with the chemical potential μ is

$$n_Q = -\left.\frac{\partial\Omega(\mu, \alpha)}{\partial\mu}\right|_{\alpha=\alpha^*}. \quad (3.4)$$

On the other hand, the pressure \mathcal{P} is a function of μ alone, $\mathcal{P}(\mu) = -\Omega(\mu, \alpha^*(\mu))$. This yields

$$\frac{d\mathcal{P}}{d\mu} = -\left[\frac{\partial\Omega}{\partial\mu} + \frac{\partial\Omega}{\partial\alpha^*} \frac{\partial\alpha^*}{\partial\mu}\right]. \quad (3.5)$$

Since $\frac{\partial\Omega}{\partial\alpha^*} = \frac{\partial\Omega}{\partial\alpha}\big|_{\alpha=\alpha^*}$ the second term in Eq. (3.5) vanishes, implying that

$$n_Q(\mu) = \frac{d\mathcal{P}}{d\mu}. \quad (3.6)$$

Finally, the energy density \mathcal{E} is given by a Legendre transform of the pressure

$$\mathcal{E}(n_Q) = -\mathcal{P}(\mu) + n_Q(\mu)\mu. \quad (3.7)$$

The solution α^* to Eq. (3.2) can also be written as a series

$$\alpha^* = \alpha_0 + \alpha_1 + \dots, \quad (3.8)$$

where α_0 is the LO solution. Expanding \mathcal{P} around α_0 , we obtain

$$\begin{aligned} \mathcal{P}(\mu) &= -\Omega(\mu, \alpha^*) = -\Omega_0(\mu, \alpha_0) - \left.\frac{\partial\Omega_0(\mu, \alpha)}{\partial\alpha}\right|_{\alpha=\alpha_0} \alpha_1 - \Omega_1(\mu, \alpha_0) + \dots \\ &= -\Omega_0(\mu, \alpha_0) - \Omega_1(\mu, \alpha_0) + \dots \end{aligned} \quad (3.9)$$

To NLO in the expansion, the pressure is given by the NLO expression for the thermodynamic potential evaluated at the LO minimum α_0 . For completeness, we show how to obtain the first correction α_1 . Eq. (3.2) is expanded as

$$\begin{aligned} 0 &= \left. \frac{\partial \Omega(\mu, \alpha)}{\partial \alpha} \right|_{\alpha=\alpha^*} \\ &= \left. \frac{\partial \Omega_0(\mu, \alpha)}{\partial \alpha} \right|_{\alpha=\alpha_0} + \left. \frac{\partial^2 \Omega_0(\mu, \alpha)}{\partial \alpha^2} \right|_{\alpha=\alpha_0} \alpha_1 + \left. \frac{\partial \Omega_1(\mu, \alpha)}{\partial \alpha} \right|_{\alpha=\alpha_0} + \dots \end{aligned} \quad (3.10)$$

Since the first term in the second line of Eq. (3.10) vanishes, we can easily find the first correction to α_0 ,

$$\alpha_1 = - \left. \frac{\partial \Omega_1}{\partial \alpha} \right|_{\alpha=\alpha_0} / \left. \frac{\partial^2 \Omega_0}{\partial \alpha^2} \right|_{\alpha=\alpha_0} . \quad (3.11)$$

4 Ground state and fluctuations at finite density

Having determined the form of the low-energy effective Lagrangian including chemical potentials, we can now discuss the form of the ground state. We also need to determine the parametrization of the fluctuations around the ground-state configuration. Once this is done, we can calculate quantum corrections to the thermodynamic potential and thereby thermodynamic quantities.

4.1 Form of the ground state

The QCD vacuum state is $\Sigma_0 = \mathbb{1}$. In order to determine the ground state at finite isospin, we consider the most general SU(2) matrix with constant fields. The most general SU(2) matrix can be parametrized as

$$\Sigma_\alpha = e^{i\hat{\phi}_a \tau_a \alpha} , \quad (4.1)$$

where α is a real parameter and $\hat{\phi}_a$ are constant fields satisfying $\hat{\phi}_a \hat{\phi}_a = 1$. The subscript α indicates that this parameter characterizes the ground state, which we will show below. Expanding the exponential and using that the Pauli matrices anticommute, Eq. (4.1) can be written as

$$\Sigma_\alpha = \mathbb{1} \cos \alpha + i \hat{\phi}_a \tau_a \sin \alpha . \quad (4.2)$$

The form of the ground state is determined by maximizing the classical thermodynamic potential Ω_0 as a function of the coefficients $\hat{\phi}_i$, or equivalently by minimizing the static Hamiltonian. The static Hamiltonian is given by $-\mathcal{L}$ evaluated for constant fields. The first term in the Lagrangian Eq. (2.18) yields the contribution denoted by $\Omega_0^{(1)}$ to the thermodynamic potential.

$$\Omega_0^{(1)} = \frac{1}{4} f^2 \langle [v_0, \Sigma^\dagger] [v_0, \Sigma] \rangle = -\frac{1}{2} f^2 \mu_I^2 (\hat{\phi}_1^2 + \hat{\phi}_2^2) \sin^2 \alpha . \quad (4.3)$$

We note that this term only depends on the sum of the square of $\hat{\phi}_1$ and $\hat{\phi}_2$. The first term Eq. (4.3) is maximized when $\hat{\phi}_1^2 + \hat{\phi}_2^2$ is as large as possible, i.e. $\hat{\phi}_3$ as small as possible due to the constraint $\hat{\phi}_a^2 = 1$. The second term reads

$$\Omega_0^{(2)} = -\frac{1}{4}f^2\langle\chi^\dagger\Sigma + \Sigma^\dagger\chi\rangle = -f^2B_0(m_u + m_d)\cos\alpha. \quad (4.4)$$

The second term term Eq. (4.4) is independent of $\hat{\phi}_a$. This implies that the thermodynamic potential is maximized for $\hat{\phi}_1^2 + \hat{\phi}_2^2 = 1$. We then write $\hat{\phi}_1 = \cos\beta$ and $\hat{\phi}_2 = \sin\beta$. We now see the competition between the two terms in the Lagrangian: The first term prefers $\sin\alpha$ as large as possible and the second term prefers $\cos\alpha$ as large as possible. The ground state is then characterized by a single parameter α and the ground state reads

$$\Sigma_\alpha = \mathbb{1}\cos\alpha + (\cos\beta\tau_1 + \sin\beta\tau_2)\sin\alpha = e^{i(\cos\beta\tau_1 + \sin\beta\tau_2)\alpha}. \quad (4.5)$$

Since the ground-state energy is independent of β , we can choose it freely and in the remainder of the paper we choose $\beta = \frac{1}{2}\pi$. The state Eq. (4.5) is a rotation of the quark condensate into a pion condensate by an angle α . The value of α as a function of μ_I is now determined by extremizing the leading-order thermodynamic potential

$$\Omega_0(\mu_I, \alpha) = -f^2m_{\pi,0}^2\cos\alpha - \frac{1}{2}f^2\mu_I^2\sin^2\alpha, \quad (4.6)$$

where $m_{\pi,0}^2 = B_0(m_u + m_d)$ is the physical mass of the charged pion at tree level (which is degenerate with the neutral pion since we have not included electromagnetic interactions yet) The solution α^* as a function of μ_I is

$$\cos\alpha^* = \begin{cases} 1, & \mu_I^2 \leq m_{\pi,0}^2, \\ \frac{m_{\pi,0}^2}{\mu_I^2}, & \mu_I^2 \geq m_{\pi,0}^2, \end{cases} \quad (4.7)$$

We next discuss the parameterization of the ground state in the three-flavor case. The most general SU(3) matrix reads

$$\Sigma_\alpha = e^{i\phi_a\lambda_a\alpha}. \quad (4.8)$$

However, since the Gell-Mann matrices do not anticommute, we can not rewrite an SU(3) in a convenient form as in the two-flavor case, Eq. (4.1). We can nevertheless use the experience in the SU(2) case to write down the form of the ground state. The hint comes from the three SU(2) subgroups of SU(3) generated by $\{\lambda_1, \lambda_2, \lambda_3\}$, $\{\lambda_4, \lambda_5, \frac{1}{2}(\lambda_3 + \sqrt{3}\lambda_8)\}$, and $\{\lambda_6, \lambda_7, \frac{1}{2}(\lambda_3 - \sqrt{3}\lambda_8)\}$. In this case, the ground state should be in the first SU(2) subgroup, corresponding to pion condensation as in the two-flavor case. Using the same arguments as above, the ground state can be written as

$$\Sigma_\alpha^{\pi^\pm} = e^{i\lambda_2\alpha} = \frac{1 + 2\cos\alpha}{3}\mathbb{1} + \frac{\cos\alpha - 1}{\sqrt{3}}\lambda_8 + i\lambda_2\sin\alpha, \quad (4.9)$$

where the superscript indicates the condensing mode. Note that, even though this state is written in terms of λ_8 , which is not a generator of the first SU(2) subgroup, this is still an

element of that group. The ground state commutes with λ_3 only for $\alpha = 0$. This means that the $U(1)_{I_3}$ symmetry is spontaneously broken in the pion-condensed phase, which by Goldstone's theorem leads to a massless excitation. Since the quark charge matrix can be written as $\frac{1}{2}(\lambda_3 + \frac{\lambda_8}{\sqrt{3}})$, the symmetry generated by the electric charge Q is also broken in this phase. In the presence of dynamical photons, this phase is a superconducting Higgs phase with a massive photon.

Similar arguments apply in the remaining cases of charged and neutral kaon condensation, as the corresponding chemical potential appears together with the generators of the remaining two $SU(2)$ subgroups. The ground states are parametrized as

$$\Sigma_\alpha^{K^\pm} = e^{i\lambda_5\alpha} = \frac{1 + 2\cos\alpha}{3}\mathbb{1} + \frac{\cos\alpha - 1}{2\sqrt{3}}\left(\sqrt{3}\lambda_3 - \lambda_8\right) + i\lambda_5\sin\alpha, \quad (4.10)$$

$$\Sigma_\alpha^{K^0/\bar{K}^0} = e^{i\lambda_7\alpha} = \frac{1 + 2\cos\alpha}{3}\mathbb{1} + \frac{1 - \cos\alpha}{2\sqrt{3}}\left(\sqrt{3}\lambda_3 + \lambda_8\right) + i\lambda_7\sin\alpha. \quad (4.11)$$

In the case of neutral kaon condensation, the phase is a superfluid, but not a superconductor. In the next section, we will use the expressions for the ground states to calculate the pressure and other thermodynamic quantities.

So far, the parametrizations we have chosen are based on our experience from the two-flavor case. We have not shown that they correspond to minima of the tree-level potential. We may verify this a posteriori by expanding in fluctuations about this point. If the linear terms vanish, this point is stationary, and if the second-order term is positive—meaning the masses are real—it is locally stable, verifying our choice. Strictly speaking, this only shows that we expand around a meta-stable state, not necessarily the global minimum. We will assume that one of the three points in $SU(3)$ we choose corresponds to the global minimum. Thus for each value of the chemical potentials, we find the ground state by evaluating which of these three points has the lowest value for the potential.

Let us finally comment on the order of the transitions from the vacuum to a Bose-condensed phase. The Bose condensate is an order parameter and in order to calculate it, we need to couple the system to an external pionic source j , cf Eq. (2.7). In the case of pion condensation, the external field becomes

$$\chi = 2B_0M + 2iB_0\lambda_2j. \quad (4.12)$$

The leading-order thermodynamic potential then reads

$$\Omega_0(\mu_I, \alpha) = -f^2B_0(m_u + m_d)\cos\alpha - f^2B_0m_s - 2f^2B_0j\sin\alpha - \frac{1}{2}f^2\mu_I^2\sin^2\alpha. \quad (4.13)$$

The quark and pion condensates are then given by the derivatives of $\Omega(\mu_I, \alpha)$ with respect to $m_{u,d}$ and j as

$$\langle\bar{q}q\rangle = \langle\bar{u}u\rangle + \langle\bar{d}d\rangle = -2f^2B_0\cos\alpha = \langle\bar{q}q\rangle_{\text{vac}}\cos\alpha, \quad (4.14)$$

$$\langle\bar{q}\gamma^5i\lambda_2q\rangle = -2f^2B_0\sin\alpha = \langle\bar{q}q\rangle_{\text{vac}}\sin\alpha. \quad (4.15)$$

We note that the sum of the square of the condensate is constant and equals the square of the quark condensate in the vacuum. Thus the quark condensate is rotated into a pion

condensate. Using $\cos \alpha = m_{\pi,0}^2/\mu_I^2$, we obtain

$$\langle \bar{u}\gamma^5 d \rangle = \langle \bar{q}q \rangle_{\text{vac}} \sqrt{1 - \frac{m_{\pi,0}^4}{\mu_I^4}}. \quad (4.16)$$

Close to the phase transition, this reduces to

$$\langle \bar{u}\gamma^5 d \rangle = 2\langle \bar{q}q \rangle_{\text{vac}} \sqrt{1 - \frac{m_{\pi,0}}{\mu_I}}. \quad (4.17)$$

Thus the order parameter is a continuous function of μ_I close to the transition, which therefore is of second order. The mean-field critical exponent is $\frac{1}{2}$, which follows directly from Eq. (4.17) and in the $O(2)$ universality class.

There is another way to see this based directly on a Ginzburg-Landau analysis of the thermodynamic potential. We expand the thermodynamic potential Eq. (4.6) in powers of α around $\alpha = 0$ to order α^4 , we obtain

$$\Omega(\mu_I, \alpha) = \frac{1}{2}f^2 [m_{\pi,0}^2 - \mu_I^2] \alpha^2 + \frac{1}{24}f^2 [4\mu_I^2 - m_{\pi,0}^2] \alpha^4. \quad (4.18)$$

A critical isospin chemical potential μ_I^c is defined by the vanishing of the quadratic term in the equation above. This yields $\mu_I^c = \pm m_{\pi,0}^2$. Since the quartic term is positive for $\mu_I = \mu_I^c$, the transition is second order. The solution of the above equation with respect to α is

$$\alpha = \sqrt{6} \sqrt{\frac{\mu_I^2 - m_{\pi,0}^2}{4\mu_I^2 - m_{\pi,0}^2}}. \quad (4.19)$$

Close to the transition, $\alpha = 2\sqrt{1 - \frac{m_{\pi,0}}{\mu_I}}$. The onset of BEC when μ_I is equal to the mass of the charged pion at tree level is a leading-order result, but is expected to hold to all orders in the low-energy expansion, where the physical pion mass is calculated in the same approximation as the thermodynamic potential. This was explicitly shown in Ref. [49] to order $\mathcal{O}(p^4)$, where the first coefficient in Eq. (4.18) is replaced by $\frac{1}{2}f_\pi^2 [m_{\pi^\pm}^2 - \mu_I^2]$, where m_{π^\pm} and f_π are now given by the NLO expressions Eqs. (6.21) and (6.23).

4.2 Fluctuations

The point Σ_α corresponds to the classical minimum for given values of μ_I and μ_S . We would like to include quantum corrections and we therefore need to discuss the parametrization of the Goldstone fields around the ground state. In the vacuum, $\alpha = 0$, we have $\Sigma = U\Sigma_0U$, where

$$U = e^{\frac{1}{2}i\lambda_a\phi_a/f}. \quad (4.20)$$

A naive way of parametrizing Σ for arbitrary α is

$$\Sigma = U\Sigma_\alpha U. \quad (4.21)$$

Using this parametrization, one can expand the Lagrangian \mathcal{L}_2 to second order in the fluctuations. It turns out that the kinetic terms are not canonically normalized so one needs

a field redefinition, which depends on the chemical potential. After the field redefinition one can calculate the NLO contribution to the thermodynamic potential arising from the functional determinant in the standard way. This contribution depends on the mass, chemical potential and angle α . The counterterms are given by the static part of the NLO Lagrangian \mathcal{L}_4 are already fixed and do not cancel the divergences for arbitrary values of α , only for the value that corresponds to the minimum of the tree-level thermodynamic potential, Eq. (4.7). In other words, we cannot renormalize the NLO thermodynamic potential away from the classical minimum and therefore not determine the value of α that minimizes it. The problem is that the parametrization Eq. (4.21) is not valid for nonzero α , which was first pointed out in Ref. [9]. Introducing

$$L_\alpha = A_\alpha U A_\alpha^\dagger, \quad R_\alpha = A_\alpha^\dagger U^\dagger A_\alpha, \quad (4.22)$$

where $A_\alpha = e^{\frac{1}{2}i\lambda_a\alpha}$ (with $a = 2, 5, 7$ depending on the ground state we consider), the correct parametrization is

$$\Sigma = L_\alpha \Sigma_\alpha R_\alpha^\dagger = A_\alpha (U \Sigma_0 U) A_\alpha. \quad (4.23)$$

This corresponds to taking the fluctuations U around the $\mu = 0$ vacuum, $\Sigma_0 = \mathbb{1}$, and applying the rotation to the new $\mu \neq 0$ ground state. Using this parametrization, the kinetic terms are automatically canonically normalized. Moreover, the $\mathcal{O}(p^4)$ counterterms cancel the ultraviolet divergences arising from the functional determinant for all values of α , as we shall see in section 6.

Using the parametrization Eq. (4.23) in the Lagrangian (2.18) and expanding in powers of the fields, we obtain $\mathcal{L}_2 = \mathcal{L}_2^{(0)} + \mathcal{L}_2^{(1)} + \dots$, where the superscript indicates the order in the fields. The zeroth-order term is exactly $-\Omega_0$ from the previous section. The linear term is

$$\mathcal{L}_2^{(1)} = f [(\mu_I^2 \cos \alpha - m_{\pi,0}^2)\phi_2 - \mu_I \partial_0 \phi_1] \sin \alpha. \quad (4.24)$$

The $\partial_0 \phi_1$ term is a total derivative and can therefore be ignored. The remaining terms vanish for $\alpha = 0$ or $\cos \alpha = m_{\pi,0}^2/\mu_I^2$, which is the criterion we found to minimize Ω_0 , implying that Σ_α is a classical solution of the equations of motion. In the next section, we calculate the masses showing that the point we expand about is a minimum. We can draw similar conclusions for the charged and neutral kaon condensates. For a given pair of μ_I and μ_S , we calculate the energy of the ground state of different phases and determine which is the global minimum and in this manner map out the phase diagram. This is also done in the next section.

We close this section with a few remarks on finite density and symmetry breaking. The conventional view is that the introduction of a chemical potential μ breaks Lorentz invariance explicitly. However, in recent years an alternative view has been put forward by Nicolis and collaborators [50, 51], namely that Lorentz invariance is broken spontaneously. At finite chemical potential μ , one uses the grand-canonical Hamiltonian defined as

$$\mathcal{H}' = \mathcal{H} - \mu Q, \quad (4.25)$$

where \mathcal{H} is the original Hamiltonian of the system and Q is the conserved charged that is a consequence of a continuous symmetry via Noether's theorem and associated with μ . We are interested in the ground state $|\mu\rangle$ of the modified Hamiltonian \mathcal{H}' , satisfying

$$\mathcal{H}'|\mu\rangle = 0. \quad (4.26)$$

If the charge Q is spontaneously broken, it follows from Eq. (4.26) that time translations (which are generated by \mathcal{H}) are also spontaneously broken since the state $|\mu\rangle$ is not an eigenstate of the original Hamiltonian \mathcal{H} . However, spatial translations are not broken, which singles out the time direction as being special. The fact that spatial translational symmetries are intact implies that the state $|\mu\rangle$ breaks all Lorentz boosts. On the other hand, a new time translation symmetry is unbroken, namely the translations generated by $\mathcal{H}' = \mathcal{H} - \mu Q$. Summarizing, all the Lorentz boosts and the internal symmetry generated by Q are all spontaneously broken, while translations (space and time), rotations and the internal symmetries not generated by Q remain unbroken. In the present case, $Q = Q_{I_3}$ is the third component of the isospin and the internal symmetry that is broken spontaneously by the Bose condensate is $U(1)_{I_3}$.⁵

The idea is that instead of doing perturbation theory around a time-independent ground state, one expands about a time-dependent ground state. We have denoted the time-independent ground state by $\Sigma_\alpha^{\pi^\pm}$. Similarly, we denote the time-dependent ground state by $\Sigma_\alpha^{\pi^\pm}(t)$, this state can be written as

$$\Sigma_\alpha^{\pi^\pm}(t) = e^{-\frac{1}{2}i\lambda_3\mu_I t} \Sigma_\alpha^{\pi^\pm} e^{\frac{1}{2}i\lambda_3\mu_I t} = e^{-\frac{1}{2}i\lambda_3\mu_I t} A_\alpha \Sigma_0 A_\alpha e^{\frac{1}{2}i\lambda_3\mu_I t}. \quad (4.27)$$

Clearly, the ground state Eq. (4.27) breaks time invariance. Hence the invariance is broken spontaneously, while the Lagrangian is Lorentz invariant. Perturbation theory is now carried out around this state with the original chiral Lagrangian with $\mu_I = 0$. This can be seen as follows. The field, now denoted by $\tilde{\Sigma}$, is parametrized around the time-dependent ground state as

$$\tilde{\Sigma} = e^{-\frac{1}{2}i\lambda_3\mu_I t} A_\alpha U \Sigma_0 U A_\alpha e^{\frac{1}{2}i\lambda_3\mu_I t}. \quad (4.28)$$

It can then be shown that

$$\partial_\mu \tilde{\Sigma} = e^{-\frac{1}{2}i\lambda_3\mu_I t} (\nabla_\mu \Sigma) e^{\frac{1}{2}i\lambda_3\mu_I t}, \quad (4.29)$$

$$\tilde{\Sigma} \chi^\dagger = e^{-\frac{1}{2}i\lambda_3\mu_I t} \Sigma \chi^\dagger e^{\frac{1}{2}i\lambda_3\mu_I t}, \quad (4.30)$$

where we have used that λ_3 and the quark mass matrix commute. Using $\partial_\mu \tilde{\Sigma}$, $\tilde{\Sigma} \chi^\dagger$ as well as their Hermitian conjugates as building blocks, together with the cyclicity of the trace, it can be seen that the resulting Lagrangian is identical to the original one.

5 Leading-order results

In this section, we derive some leading-order results, namely the quasiparticle masses in the pion-condensed phase, pressure, densities (isospin and strangeness), and the phase diagram in the $\mu_I - \mu_S$ plane.

⁵We consider here a pion condensate, similar results are obtained for the kaon-condensed phases.

5.1 Quasiparticle masses

In order to calculate the dispersion relations for the quasiparticles, we expand the LO Lagrangian to second order in the fields. We do this in the pion-condensed phase, similar results can be obtained for the kaon-condensed phases. For simplicity, we consider the isospin limit and $\mu_S = 0$. The quadratic terms are

$$\begin{aligned} \mathcal{L}_2^{(2)} = & -\frac{1}{4}F_{\mu\nu}F^{\mu\nu} + \frac{1}{2}m_A^2\eta_{\mu\nu}A^\mu A^\nu + \frac{1}{2}\partial_\mu\phi_a\partial^\mu\phi_a + \frac{1}{2}m_{ab}\phi_a\partial_0\phi_b - m_{\phi A}^2\phi_2A^0 \\ & -\frac{1}{2}m_a^2\phi_a^2 - \frac{1}{\sqrt{3}}\Delta m^2\phi_3\phi_8 + \partial_\mu\bar{c}\partial^\mu c - m_c^2\bar{c}c + \frac{1}{2\xi}(\partial_\mu A^\mu)^2. \end{aligned} \quad (5.1)$$

Here, we have introduced a number of mass parameters, which will in general be functions of α and the chemical potentials. Including electromagnetic effects, the diagonal mass terms are

$$m_1^2 = m_{\pi,0}^2 \cos \alpha - (\mu_I^2 - \Delta m_{\text{EM}}^2) \cos^2 \alpha + \xi e^2 f^2 \sin^2 \alpha, \quad (5.2)$$

$$m_2^2 = m_{\pi,0}^2 \cos \alpha - (\mu_I^2 - \Delta m_{\text{EM}}^2) \cos 2\alpha, \quad (5.3)$$

$$m_3^2 = m_{\pi,0}^2 \cos \alpha + (\mu_I^2 - \Delta m_{\text{EM}}^2) \sin^2 \alpha, \quad (5.4)$$

$$m_4^2 = m_{K^\pm,0}^2 + \frac{1}{2}m_{\pi,0}^2(\cos \alpha - 1) - \frac{1}{4}\mu_I^2 \cos 2\alpha + \frac{1}{2}\Delta m_{\text{EM}}^2 \cos \alpha(\cos \alpha + 1), \quad (5.5)$$

$$m_6^2 = m_{K^0,0}^2 + \frac{1}{2}m_{\pi,0}^2(\cos \alpha - 1) - \frac{1}{4}\mu_I^2 \cos 2\alpha + \frac{1}{2}\Delta m_{\text{EM}}^2 \cos \alpha(\cos \alpha - 1), \quad (5.6)$$

$$m_8^2 = m_{\eta,0}^2 + \frac{1}{3}m_{\pi,0}^2(\cos \alpha - 1), \quad (5.7)$$

$$m_A^2 = e^2 f^2 \sin^2 \alpha, \quad (5.8)$$

$$m_c^2 = \xi e^2 f^2 \sin^2 \alpha. \quad (5.9)$$

In addition, $m_6^2 = m_7^2$ and $m_4^2 = m_5^2$. The nonvanishing off-diagonal terms are

$$m_{12} = 2\mu_I \cos \alpha, \quad (5.10)$$

$$m_{45} = \mu_I \cos \alpha, \quad (5.11)$$

$$m_{67} = -\mu_I \cos \alpha, \quad (5.12)$$

and $m_{ab} = -m_{ba}$. The coupling between ϕ_2 and A^0 is

$$m_{\phi A}^2 = e f \mu_I \sin 2\alpha, \quad (5.13)$$

The quark masses are related to the quantities introduced in Eq. (5.2)–(5.7)

$$m_{\pi,0}^2 = B_0(m_u + m_d), \quad m_{K^0,0}^2 = B_0(m_d + m_s), \quad (5.14)$$

$$m_{K^\pm,0}^2 = B_0(m_u + m_s), \quad m_{\eta,0}^2 = \frac{1}{3}B_0(m_u + m_d + 4m_s), \quad (5.15)$$

$$\Delta m^2 = B_0(m_d - m_u), \quad \Delta m_{\text{EM}}^2 = \frac{2Ce^2}{f^2}. \quad (5.16)$$

This is an overconstrained system of equations, with $3m_{\eta,0}^2 = 2m_{K^\pm,0}^2 + 2m_{K^0,0}^2 - m_{\pi,0}^2$ and $m_{K^0,0}^2 - m_{K^\pm,0}^2 = \Delta m^2$. In the isospin limit $\Delta m^2 = 0$ and in the vacuum, the off-diagonal

terms vanish. We identify $m_1^2 = m_2^2 = m_{\pi,0}^2 + \Delta m_{\text{EM}}^2$ with the masses of the charged pions, $m_3^2 = m_{\pi,0}^2$ with the neutral pion, and so on.

Outside this limit, the physical masses are given by the poles of the full propagator, which has a complicated form due to off-diagonal terms that will lead to mixing. Note that the ghost decouples completely and its tree-level mass is given by Eq. (5.9). We may write the Lagrangian compactly as

$$\mathcal{L}_2^{(2)} = \frac{1}{2} \psi_i D_{ij}^{-1} \psi_j + \partial_\mu \bar{c} \partial^\mu c - m_c^2 \bar{c} c, \quad (5.17)$$

where we have combined the fields into a twelve-component vector, $\psi_i = (\phi_a, A_\mu)$, where the index $i \in \{1, \dots, 8\}$ corresponds to the mesonic field subscript a , while $i \in \{9, \dots, 12\}$ corresponds to the Lorentz index μ of the photon field. We write the inverse propagator as a matrix composed of four blocks

$$D_{ij}^{-1}(\omega, p) = \begin{pmatrix} D_{\phi\phi}^{-1} & D_{\phi A}^{-1} \\ D_{A\phi}^{-1} & D_{AA}^{-1} \end{pmatrix}, \quad (5.18)$$

where $D_{\phi A}^{-1} = D_{A\phi}^{-1}$. The meson part $D_{\phi\phi}^{-1}$ can further be written in block-diagonal form, plus a $\pi_0 - \eta$ mixing term

$$D_{\phi\phi}^{-1}(\omega, p) = \begin{pmatrix} D_{12}^{-1} & & & \\ & \omega^2 - p^2 - m_3^2 & & \\ & & D_{45}^{-1} & \\ & & & D_{67}^{-1} \\ & & & & \omega^2 - p^2 - m_8^2 \end{pmatrix} + \Delta D^{-1}. \quad (5.19)$$

The three blocks all have the same form,

$$D_{ij}^{-1}(\omega, p) = \begin{pmatrix} \omega^2 - p^2 - m_i^2 & -i\omega m_{ij} \\ -i\omega m_{ji} & \omega^2 - p^2 - m_j^2 \end{pmatrix}, \quad (5.20)$$

while the only nonzero elements of the matrix ΔD^{-1} are

$$\Delta D_{38}^{-1} = \Delta D_{83}^{-1} = -\frac{1}{\sqrt{3}} \Delta m^2. \quad (5.21)$$

The spectrum is now given by the zeros of the determinant of the inverse propagator, $\det [D^{-1}(\omega, p)] = 0$ is solved for $E = \omega$. We first consider the case without electromagnetic effects, $e = 0$. The spectra of the mesons are

$$E_{\pi^0/\eta}^2 = p^2 + \frac{1}{2} (m_3^2 + m_8^2) \mp \frac{1}{2\sqrt{3}} \sqrt{3(m_3^2 - m_8^2)^2 + 4(\Delta m^2)^2}, \quad (5.22)$$

$$E_{\bar{\pi}^\pm}^2 = p^2 + \frac{1}{2} (m_1^2 + m_2^2 + m_{12}^2) \mp \frac{1}{2} \sqrt{4p^2 m_{12}^2 + (m_1^2 + m_2^2 + m_{12}^2)^2 - 4m_1^2 m_2^2}, \quad (5.23)$$

$$E_{\bar{K}^\pm}^2 = p^2 + m_4^2 + \frac{1}{2} m_{45}^2 \mp \frac{1}{2} m_{45} \sqrt{4p^2 + 4m_4^2 + m_{45}^2}, \quad (5.24)$$

$$E_{\bar{K}^0/\bar{K}^0}^2 = p^2 + m_6^2 + \frac{1}{2} m_{67}^2 \pm \frac{1}{2} m_{67} \sqrt{4p^2 + 4m_6^2 + m_{67}^2}. \quad (5.25)$$

The modes in Eqs. (5.22) are identified with the neutral pion and the η . The modes in Eq. (5.23) are linear combinations of π^+ and π^- , denoted by a $\tilde{\pi}^\pm$. At onset of pion condensation, $\tilde{\pi}^+$ coincides with π^+ and $\tilde{\pi}^-$ coincides with π^- . Similar remarks apply to the kaon modes, Eqs. (5.24) and (5.25). The effective masses of the particle are then given by $m = E(p = 0)$.

We now consider the full propagator, choosing the Feynman-'t Hooft gauge, $\xi = 1$, to perform the calculations. The photon propagator then becomes diagonal, and is given by

$$(D_{AA}^{-1})_{\mu\nu} = \eta_{\mu\nu}(m_A^2 - \omega^2 + p^2). \quad (5.26)$$

The coupling between the mesons and the photon is

$$(D_{\phi A}^{-1})_{2,0} = -m_{\phi A}^2. \quad (5.27)$$

With this, we can calculate the complete spectrum of the system. However, due to the complicated expressions we will not list them, only the quasiparticle masses will be given. In the last section, we found that the transition to the symmetry-broken phase happens at $\mu_I^2 = m_{\pi,0}^2$. When electromagnetic effects are included, the transition point is changed to $\mu_{I,\text{eff}}^2 = \mu_I^2 - \Delta m_{\text{EM}}^2 = m_{\pi,0}^2$, or $\mu_I^2 = m_{\pi^\pm,0}^2$, (see details in subsec. 5.3). For $\mu_{I,\text{eff}} \leq m_{\pi,0}$, $\alpha = 0$, and as a result the mass of the photon vanishes. The remaining masses in the symmetric phase are

$$m_{\pi^0/\eta}^2 = \frac{1}{3} \left(m_{K^\pm,0}^2 + m_{K^0,0}^2 + m_{\pi,0}^2 \mp \sqrt{(m_{K^\pm,0}^2 + m_{K^0,0}^2 - 2m_{\pi,0}^2)^2 + 3(\Delta m^2)^2} \right), \quad (5.28)$$

$$m_{\tilde{\pi}^\pm}^2 = \left(\sqrt{m_{\pi,0}^2 + \Delta m_{\text{EM}}^2} \mp \mu_I \right)^2, \quad (5.29)$$

$$m_{\tilde{K}^0/\tilde{K}^0}^2 = \left(m_{K^0,0} \mp \frac{1}{2}\mu_I \right)^2, \quad (5.30)$$

$$m_{\tilde{K}^\pm}^2 = \left(\sqrt{m_{K^\pm,0}^2 + \Delta m_{\text{EM}}^2} \mp \frac{1}{2}\mu_I \right)^2. \quad (5.31)$$

For $\mu_{I,\text{eff}} \geq m_{\pi,0}$, the exact $U(1)$ symmetry generated by λ_3 is broken. When we exclude electromagnetic interactions, the positive pion becomes a Goldstone boson in the broken phase. However, as the generator of electric charge is given by $\lambda_Q = \lambda_3 + \frac{1}{\sqrt{3}}\lambda_8$, this symmetry is a gauge symmetry, which cannot be broken. The positive pion disappears from the spectrum and this degree of freedom is ‘‘eaten’’ by the photon via the Higgs mechanism. As a result, the photon becomes massive with three polarization states. In the symmetry broken phase, we have $\cos \alpha_0 = m_{\pi,0}^2/\mu_{I,\text{eff}}^2$. Using this, the various masses are, denoting $\tilde{m}^2 = \frac{2}{3}(m_{K^\pm,0}^2 + m_{K^0,0}^2 - m_{\pi,0}^2)$,

$$m_{\pi^0/\eta}^2 = \frac{1}{2}(\tilde{m}^2 + \mu_{I,\text{eff}}^2) + \frac{m_{\pi,0}^4}{6\mu_{I,\text{eff}}^2} \mp \frac{1}{6\mu_{I,\text{eff}}^2} \sqrt{12(\Delta m^2)^2 \mu_{I,\text{eff}}^4 + [3\mu_{I,\text{eff}}^2(\tilde{m}^2 - \mu_{I,\text{eff}}^2) + m_{\pi,0}^4]^2}, \quad (5.32)$$

$$\begin{aligned}
m_{\tilde{K}^0/\tilde{K}^{\pm}}^2 &= m_{K^0,0}^2 + \frac{1}{4}\mu_I^2 + \frac{m_{\pi,0}^2\mu_I^2(m_{\pi,0}^2 - \mu_{I,\text{eff}}^2)}{2\mu_{I,\text{eff}}^4} \\
&\mp \frac{m_{\pi,0}^2|\mu_I|}{2\mu_{I,\text{eff}}^4} \sqrt{\mu_I^2 m_{\pi,0}^4 + \mu_{I,\text{eff}}^2 [\mu_I^2 (\mu_{I,\text{eff}}^2 - 2m_{\pi,0}^2) + 4m_{K^0,0}^2 \mu_{I,\text{eff}}^2]} , \quad (5.33)
\end{aligned}$$

$$\begin{aligned}
m_{K^\pm}^2 &= m_{K^\pm,0}^2 + \frac{1}{4}\mu_I^2 + \frac{m_{\pi,0}^2}{2\mu_{I,\text{eff}}^4} [\mu_I^2 m_{\pi,0}^2 - \mu_{I,\text{eff}}^2 (\mu_{I,\text{eff}}^2 - \Delta m_{\text{EM}}^2)] \mp \frac{m_{\pi,0}^2|\mu_I|}{2\mu_{I,\text{eff}}^4} \\
&\times \sqrt{\mu_I^2 m_{\pi,0}^4 + \mu_{I,\text{eff}}^2 [\mu_I^2 (\mu_{I,\text{eff}}^2 - 2m_{\pi,0}^2) + 4m_{K^\pm,0}^2 \mu_{I,\text{eff}}^2 + 4\Delta m_{\text{EM}}^2 m_{\pi,0}^2]} , \quad (5.34)
\end{aligned}$$

$$m_{\pi^-}^2 = \mu_{I,\text{eff}}^2 \left[1 + \frac{m_{\pi,0}^4 (3\mu_{I,\text{eff}}^2 + 4\Delta m_{\text{EM}}^2)}{\mu_{I,\text{eff}}^6} \right] , \quad (5.35)$$

$$m_A^2 = e^2 f^2 \left[1 - \frac{m_{\pi,0}^2}{\mu_{I,\text{eff}}^2} \right] . \quad (5.36)$$

The masses are plotted, as functions of isospin chemical potential, in Fig. 3. How to connect the bare parameters to physical observables and thus obtain numerical results is discussed below. We see that the masses are continuous functions of the chemical potential, but they are nondifferentiable across the symmetry breaking point.

At some point, the masses of the neutral pion and η approach each other, as illustrated in Fig. 4. This happens as the second term in the root vanishes. If $\Delta m^2 = 0$, the root term vanishes and the absolute value leads to nondifferentiable behavior as the lines intersect, while for $\Delta m^2 \neq 0$ the lines are smooth and never overlap. Above this point, the two masses “change roles”, as the neutral pion mass approaches a constant, while the η mass grows linearly.

5.2 Connection to physical observables

The masses given above are the physical pole masses at tree level and identified with the observed masses. The measured values are taken from the Particle Data Group [52] together with the experimental value of the pion-decay constant,

$$\begin{aligned}
m_{\pi^0} &= 134.98 \text{ MeV} , & m_{\pi^\pm} &= 139.57 \text{ MeV} , \\
m_{K^\pm} &= 493.68 \text{ MeV} , & m_{K^0} &= 497.61 \text{ MeV} .
\end{aligned}$$

At $\mu_I = 0$, we get from Eqs. (5.28)–(5.31), using $m_{K^0,0}^2 = m_{K^\pm,0}^2 + \Delta m^2$,

$$3m_{\pi^0}^2 = 2m_{K^\pm,0}^2 + m_{\pi,0}^2 + \Delta m^2 - \sqrt{(2m_{K^\pm,0}^2 - 2m_{\pi,0}^2 + \Delta m^2)^2 + 3\Delta m^4} , \quad (5.37)$$

$$m_{\pi^\pm}^2 = m_{\pi,0}^2 + \Delta m_{\text{EM}}^2 , \quad (5.38)$$

$$m_{K^0}^2 = m_{K^\pm,0}^2 + \Delta m^2 , \quad (5.39)$$

$$m_{K^\pm}^2 = m_{K^\pm,0}^2 + \Delta m_{\text{EM}}^2 . \quad (5.40)$$

Solving these numerically with the values given above, we obtain

$$m_{\pi,0} = 135.09 \text{ MeV} , \quad m_{K^\pm,0} = 492.43 \text{ MeV} , \quad (5.41)$$

$$\Delta m^2 = (71.60 \text{ MeV})^2 , \quad \Delta m_{\text{EM}}^2 = (35.09 \text{ MeV})^2 . \quad (5.42)$$

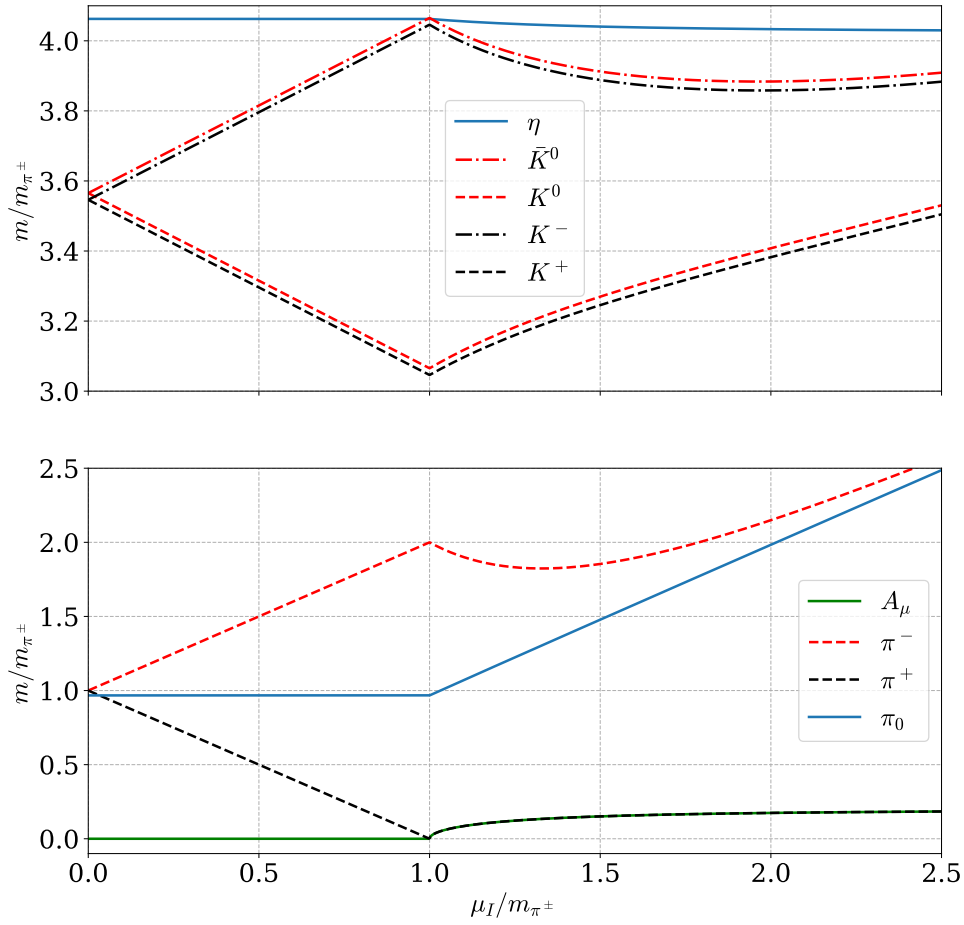


Figure 3. Quasi-particle masses at leading order in χ PT as functions of the isospin chemical potential μ_I normalized to $m_{\pi,0}$. See main text for details.

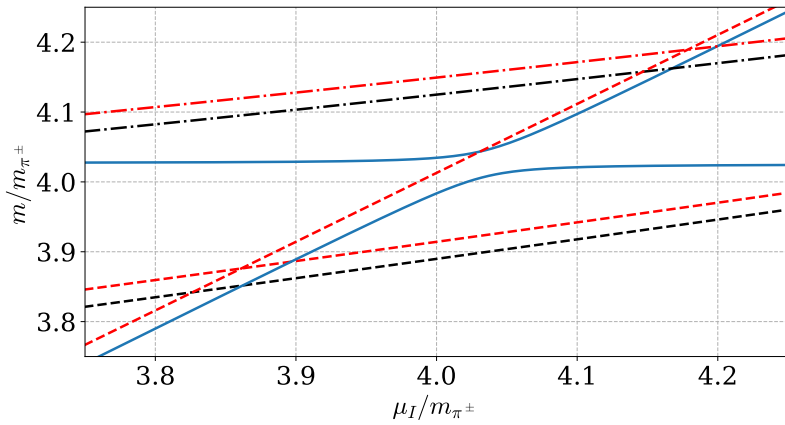


Figure 4. The masses of the π^0 and the η approach each other before “changing roles”, as described in the main text.

The mass splittings between neutral and charge mesons have two sources. The first arises from the electromagnetic interactions, $\Delta m_{\text{EM}}^2 = \frac{2Ce^2}{f^2}$, which is the same for pions and kaons. This is Dashen's theorem [35]. Using the values for the pion masses above and the decay constant and electromagnetic coupling from [52],

$$f_\pi = 92.07\text{MeV}, \quad e = 0.3028, \quad (5.43)$$

we find that the coupling introduced by Urech is

$$C = \frac{f^2}{2e^2} \Delta m_{\text{EM}}^2 = 5.692 \times 10^{-5} (\text{GeV})^4. \quad (5.44)$$

We note in passing that the constant C can be expressed in terms of the mass of the ρ meson, its decay constant f_ρ , and f_π as [53]

$$C = \frac{3m_\rho^2 f_\rho^2}{2(4\pi)^2} \ln \left(\frac{f_\rho^2}{f_\rho^2 - f_\pi^2} \right). \quad (5.45)$$

Using the values $f_\pi = 93.3 \text{ MeV}$, $f_\rho = 154 \text{ MeV}$ and $m_\rho = 770 \text{ MeV}$, Urech obtains the numerical result $6.11 \times 10^{-5} (\text{GeV})^4$.

The second source of mass splitting is the mass difference between the u and the d quark, encoded in Δm^2 . For the pion this takes a more complicated form, due to the mixing of π^0 and η . To leading order in Δm^2 ,

$$m_{\pi^0}^2 = m_{\pi,0}^2 - \frac{1}{4} \frac{(\Delta m^2)^2}{m_{K^\pm,0}^2 - m_{\pi,0}^2} + \mathcal{O}((\Delta m^2)^3). \quad (5.46)$$

Therefore, $m_{\pi^\pm}^2 = m_{\pi,0}^2 + \Delta m_{\text{EM}}^2 + \mathcal{O}((\Delta m^2)^2)$, and the mass splitting of the neutral and charged pion is dominated by the electromagnetic contribution. For the kaon, on the other hand, the contributions are of the same order. Notice that the corrections pull in opposite directions,

$$m_{K^\pm}^2 = m_{K^0}^2 - \Delta m^2 + \Delta m_{\text{EM}}^2, \quad (5.47)$$

decreasing the absolute value of the mass splitting.

5.3 Phase diagram

In this section, we calculate the pressure \mathcal{P} and present the phase diagram at $T = 0$ in the $\mu_I - \mu_S$ plane for three-flavor χ PT including electromagnetic effects. The leading-order thermodynamic potential in the pion-condensed phase is

$$\Omega_0(\mu_I, \alpha) = -f^2 \left[m_{\pi,0}^2 \cos \alpha + B_0 m_s + \frac{2}{3} \Delta m_{\text{EM}}^2 + \frac{1}{2} (\mu_I^2 - \Delta m_{\text{EM}}^2) \sin^2 \alpha \right], \quad (5.48)$$

where we have used the form of the ground state $\Sigma_\alpha^{\pi^\pm}$ given in Eq. (4.9). The value α that extremizes $\Omega_0(\mu_I, \alpha)$ satisfies

$$\cos \alpha_0 = \frac{B_0(m_u + m_d)}{\mu_I^2 - \Delta m_{\text{EM}}^2} = \frac{m_{\pi,0}^2}{\mu_{I,\text{eff}}^2}, \quad (5.49)$$

valid for $\mu_{I,\text{eff}}^2 = \mu_I^2 - \Delta m_{\text{EM}}^2 \geq m_{\pi,0}^2$. The transition therefore takes place at $\mu_{I,\text{eff}}^2 = m_{\pi,0}^2$, which is equivalent to $\mu_I^2 = m_{\pi^\pm}^2 = m_{\pi,0}^2 + \Delta m_{\text{EM}}^2$, i.e. the tree-level mass of the condensing charged pion. The pressure is expressed as $\mathcal{P}(\mu_I) = -\Omega_0(\mu_I, \alpha_0)$. Subtracting the pressure in the vacuum phase, we obtain

$$\mathcal{P} = \frac{1}{2} f^2 \mu_{I,\text{eff}}^2 \left[1 - \frac{m_{\pi,0}^2}{\mu_{I,\text{eff}}^2} \right]^2. \quad (5.50)$$

In the pion-condensed phase, the isospin and strangeness densities n_I and n_S are obtained from $n_Q = \frac{d\mathcal{P}}{d\mu_Q}$, which gives

$$n_I = f^2 \mu_I \left[1 - \frac{m_{\pi,0}^4}{\mu_{I,\text{eff}}^4} \right], \quad n_S = 0. \quad (5.51)$$

We note that the leading-order results for the pion-condensed phase, Eqs. (5.50)–(5.51), are independent of m_s and are identical to the results in two-flavor χ PT

The pressure and the densities of the other phases can be calculated in the same way, using the corresponding parametrization of the ground states $\Sigma_\alpha^{K^\pm}$ and $\Sigma_\alpha^{K^0/\bar{K}^0}$. In the charged kaon condensed phase, we obtain

$$\mathcal{P} = \frac{1}{2} f^2 \mu_{K^\pm,\text{eff}}^2 \left[1 - \frac{m_{K^\pm,0}^2}{\mu_{K^\pm,\text{eff}}^2} \right]^2, \quad n_I = \frac{1}{2} n_S = -\frac{1}{2} f^2 \mu_{K^\pm} \left[1 - \frac{m_{K^\pm,0}^4}{\mu_{K^\pm,\text{eff}}^4} \right], \quad (5.52)$$

where $\mu_{K^\pm,\text{eff}}^2 = \mu_{K^\pm}^2 - \Delta m_{\text{EM}}^2$. Finally, in the neutral kaon condensed phase, we find

$$\mathcal{P} = \frac{1}{2} f^2 \mu_{K^0}^2 \left[1 - \frac{m_{K^0,0}^2}{\mu_{K^0}^2} \right]^2, \quad n_I = -\frac{1}{2} n_S = \frac{1}{2} f^2 \mu_{K^0} \left[1 - \frac{m_{K^0,0}^4}{\mu_{K^0}^4} \right]. \quad (5.53)$$

In order to find the transition line between the condensed phases, we equate the pressure of the two phases. This gives rise to a line in the phase diagram, which can be solved for one of the chemical potentials as a function of the other chemical potential and the vacuum masses of the condensing modes in adjacent phases. For example, the line between the charged condensed phases satisfies

$$\mu_{K^\pm,\text{eff}} = \frac{1}{2\mu_{I,\text{eff}}} \left(\mu_{I,\text{eff}}^2 - m_{\pi,0}^2 + \sqrt{(\mu_{I,\text{eff}}^2 - m_{\pi,0}^2)^2 + 4\mu_{I,\text{eff}}^2 m_{K^\pm,0}^2} \right). \quad (5.54)$$

In Fig. 5, we show the phase diagram in the μ_I – μ_S plane at zero temperature (left panel) and the details near the triple points (right panel). The black lines are without electromagnetic effects and in obtaining the red lines they are included. Solid lines separating the phases indicate that the transition is second order, while dotted lines indicate a first-order transition. In the isospin limit ($m_u = m_d$), this phase diagram was first obtained in Ref. [10]. All the transition from the vacuum phase are second order as we have already demonstrated in the transition to the pion-condensed phase. The transitions are in the $O(2)$ universality class with mean-field exponents. The transitions between the different condensed phases are first order. This can be seen either by a jump in the relevant

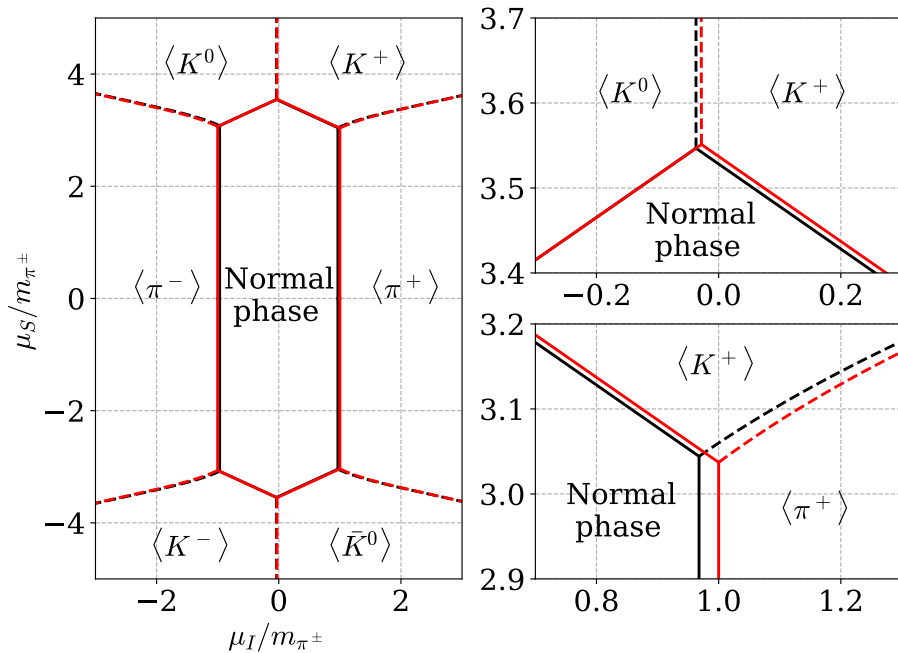


Figure 5. Left panel: Tree-level phase diagram in the $\mu_I - \mu_S$ plane. Right panel: zoom in on the tricritical points. See main text for details.

condensates or by a discontinuity in the relevant rotation angles. The points where three phases meet (six points) are the triple points. In the right panel, we notice the small offset between the black and red lines. Since we normalize the chemical potentials to the mass of the charged pion, the lines indicating the onset of charge meson condensation move upon including electromagnetic effects. For example, the vertical line separating the vacuum and the pion-condensed phase is now at

$$\frac{\mu_I^c}{m_{\pi^0,0}} = \frac{m_{\pi^\pm}}{m_{\pi^0,0}} = \sqrt{1 + \frac{\Delta m_{\text{EM}}^2}{m_{\pi^0,0}^2}}. \quad (5.55)$$

Finally, we notice that the normal phase is independent of the chemical potentials, and so the pressure is constant and the densities vanish in the entire region. This is an example of the so-called Silver Blaze property [23]. More generally, the properties of a specific Bose-condensed phase depends only on a single chemical potential, namely the relevant one, μ_I , μ_{K^\pm} , or μ_{K^0} .

6 Thermodynamics at next-to-leading order

In this section, we calculate the pressure at next-to-leading order in the low-energy expansion in the pion-condensed phase. One can obtain similar results for the two kaon-condensed phases. In order to simplify the calculations and to compare our results with lattice simulations, we work in the isospin limit, $m_u = m_d$, and ignore electromagnetic effects. From the pressure, we calculate other interesting quantities such as the speed of sound, isospin density, and energy density.

6.1 Thermodynamic potential and pressure

There are two contributions to the next-leading order thermodynamic potential, namely the static term from \mathcal{L}_4 and the one-loop contribution from \mathcal{L}_2 . The first term reads

$$\begin{aligned}\Omega_1^{(1)}(\mu_I, \alpha) = & -(4L_1 + 4L_2 + 2L_3)\mu_I^4 \sin^4 \alpha - 8L_4 B_0(2m \cos \alpha + m_s)\mu_I^2 \sin^2 \alpha \\ & - 8L_5 B_0 m \mu_I^2 \cos \alpha \sin^2 \alpha - 16L_6 B_0^2(2m \cos \alpha + m_s)^2 \\ & - 8L_8 B_0^2(2m^2 \cos 2\alpha + m_s^2) - 4H_2 B_0^2(2m^2 + m_s^2),\end{aligned}\quad (6.1)$$

where we denote $m = m_u = m_d$.

The one-loop contribution from the quasiparticles is given by

$$\begin{aligned}\Omega_1^{(2)}(\mu_I, \alpha) = & \frac{1}{2} \int_P \log [p_0^2 + E_{\pi^0}(p)^2] + \int_P \log [p_0^2 + E_{\bar{\pi}^\pm}(p)^2] + \int_P \log [p_0^2 + E_{\bar{K}^\pm}(p)^2] \\ & + \int_P \log [p_0^2 + E_{\bar{K}^0/\bar{K}^0}(p)^2] + \frac{1}{2} \int_P \log [p_0^2 + E_\eta(p)^2],\end{aligned}\quad (6.2)$$

where the dispersion relations are given by Eqs. (5.22)–(5.25), again with $\Delta m_{\text{EM}}^2 = 0$, and we denote the Euclidean four-momentum by $P^2 = p_0^2 + p^2$. The shorthand for the integral is defined in Appendix A. The first and the last term in Eq. (6.2) are of the form Eq. (A.7). Interestingly, the integrals involving the charged and neutral kaons can also be evaluated directly in dimensional regularization as $m_4 = m_5$. Combining the two contributions from the charged kaons, we find

$$\begin{aligned}\Omega_{1,K^\pm}^{(2)}(\mu_I, \alpha) = & \frac{1}{2} \int_P \log [(P^2 + m_4^2)(P^2 + m_5^2) + p_0^2 m_{45}^2] \\ = & \frac{1}{2} \int_P \log \left[\left(p_0 + \frac{i m_{45}}{2} \right)^2 + p^2 + m_4^2 + \frac{1}{4} m_{45}^2 \right] \\ & \times \left[\left(p_0 - \frac{i m_{45}}{2} \right)^2 + p^2 + m_4^2 + \frac{1}{4} m_{45}^2 \right],\end{aligned}\quad (6.3)$$

where we in the second line have used $m_4 = m_5$ and factorized. Shifting the integration variable p_0 in the two terms, $p_0 \rightarrow p_0 \pm \frac{i}{2} m_{45}$, we obtain

$$\Omega_{1,K^\pm}^{(2)}(\mu_I, \alpha) = \int_P \log [P^2 + \tilde{m}_4^2], \quad (6.4)$$

where we have defined $\tilde{m}_4^2 = m_4^2 + \frac{1}{4} m_{45}^2$. The contribution from the neutral kaons is given by the same expression with the replacement $m_6^2 = m_7^2 \rightarrow \tilde{m}_6^2 = m_6^2 + \frac{1}{4} m_{67}^2$. Finally, consider the contribution from the charged pions. We first rewrite their contribution in the same way as for the charged kaons in Eq. (6.3),

$$\Omega_{1,\pi^\pm}^{(2)}(\mu_I, \alpha) = \frac{1}{2} \int_P \log [(P^2 + m_1^2)(P^2 + m_2^2) + p_0^2 m_{12}^2]. \quad (6.5)$$

Since $m_1 \neq m_2$, we cannot factorize this expression as we did above. Eq. (6.5) can thus not be evaluated directly in dimensional regularization. However, using the techniques from

Ref. [54], we extract the divergences and express the remainder in terms of a hypergeometric function. Since $m_1 = 0$ at leading order, the contribution to the pressure is

$$\begin{aligned}\Omega_{1,\pi^\pm}^{(2)}(\mu_I, \alpha) &= \frac{1}{2} \int_P \log [P^2(P^2 + m_2^2) + p_0^2 m_{12}^2] \\ &= \frac{1}{2} \int_P \log [P^2 + m_2^2] - \frac{1}{2} \sum_{n=1}^{\infty} \frac{(-1)^n m_{12}^{2n}}{n} \int_P \frac{p_0^{2n}}{P^{2n}(P^2 + m_2^2)^n},\end{aligned}\quad (6.6)$$

where we in the second line have expanded the logarithm in powers of the dimensionless variable $z = m_{12}^2/m_2^2$. Averaging Eq. (6.6) over angles, we find

$$\Omega_{1,\pi^\pm}^{(2)}(\mu_I, \alpha) = -\frac{1}{2} I_0'(m_2^2) - \frac{\Gamma(2-\epsilon)}{2\Gamma(\frac{1}{2})} \sum_{n=1}^{\infty} \frac{\Gamma(n+\frac{1}{2})}{\Gamma(n+2-\epsilon)} \frac{(-1)^n m_{12}^{2n}}{n} I_n(m_2^2),\quad (6.7)$$

where the integrals $I_0'(m_2^2)$ and $I_n(m_2^2)$ are defined in Eqs. (A.3)–(A.4). We single out the divergent terms in the series ($n = 1, 2$) and set $d = 3$ in the remainder ($n \geq 3$). Redefining the dummy index n and introducing the Pochhammer symbol $(a)_b = \Gamma[a+b]/\Gamma[a]$, we can write

$$\begin{aligned}\Omega_{1,\pi^\pm}^{(2)}(\mu_I, \alpha) &= -\frac{1}{2} I_0'(m_2^2) + \frac{m_{12}^2}{2(d+1)} I_1(m_2^2) - \frac{3m_{12}^4}{4(d+1)(d+3)} I_2(m_2^2) \\ &\quad + \frac{5m_{12}^6}{768(4\pi)^2 m_2^2} \sum_{n=0}^{\infty} \frac{(1)_n (1)_n (\frac{7}{2})_n}{(5)_n (4)_n} \frac{(-\frac{m_{12}^2}{m_2^2})^n}{n!}.\end{aligned}\quad (6.8)$$

The series identified as the series expansion of a hypergeometric function ${}_3F_2$ [55], and so we obtain

$$\begin{aligned}\Omega_{1,\pi^\pm}^{(2)}(\mu_I, \alpha) &= -\frac{1}{2} I_0'(m_2^2) + \frac{m_{12}^2}{2(d+1)} I_1(m_2^2) - \frac{3m_{12}^4}{4(d+1)(d+3)} I_2(m_2^2) \\ &\quad + \frac{5m_{12}^6}{768(4\pi)^2 m_2^2} {}_3F_2 \left[\begin{matrix} 1, & 1, & \frac{7}{2} \\ & 4, & 5 \end{matrix} \middle| -\frac{m_{12}^2}{m_2^2} \right].\end{aligned}\quad (6.9)$$

The hypergeometric function ${}_3F_2$ has a closed-form expression

$$\begin{aligned}{}_3F_2 \left[\begin{matrix} 1, & 1, & \frac{7}{2} \\ & 4, & 5 \end{matrix} \middle| z \right] &= \frac{16}{5} \left[\frac{(3z^2 - 10z - 8)(1 - \sqrt{1-z})}{z^4} + \frac{z^2 + 4}{z^3} \right. \\ &\quad \left. - 3 \frac{z^2 - 4z + 8}{z^3} \log \frac{1 + \sqrt{1-z}}{2} \right].\end{aligned}\quad (6.10)$$

Adding the contributions, renormalizing the bare couplings according to Eq. (2.23), and evaluating the expressions for $\cos \alpha^* = \frac{m_{\pi,0}^2}{\mu_I^2}$ we obtain the next-to-leading order pressure. In the final result, we subtract the vacuum pressure. This yields

$$\begin{aligned}\mathcal{P}_{0+1} &= \frac{1}{2} f^2 \mu_I^2 \left[1 - \frac{m_\pi^2}{\mu_I^2} \right] - \frac{1}{2} f^2 \frac{m_{\pi,0}^4}{m_\pi^2} \left[1 - \frac{m_\pi^2}{\mu_I^2} \right] \\ &\quad + \left[4L_1^r + 4L_2^r + 2L_3^r + \frac{1}{4(4\pi)^2} \left(\log \frac{\Lambda^2}{m_2^2} + \log \frac{\Lambda^2}{m_3^2} + \frac{1}{4} \log \frac{\Lambda^2}{\tilde{m}_4^2} + \frac{9}{8} \right) \right] \mu_I^4\end{aligned}$$

$$\begin{aligned}
& - \left[32L_6^r + \frac{1}{(4\pi)^2} \left(\log \frac{\Lambda^2}{m_{K,0}^2} + \frac{2}{9} \log \frac{\Lambda^2}{m_{\eta,0}^2} + \frac{11}{18} \right) \right] m_{\pi,0}^2 \tilde{m}_{K,0}^2 \\
& - \left[8L_1^r + 8L_2^r + 4L_3^r - 8L_4^r - 4L_5^r + 16L_6^r + 8L_8^r \right. \\
& \left. + \frac{1}{4(4\pi)^2} \left(3 \log \frac{\Lambda^2}{m_{\pi,0}^2} + \log \frac{\Lambda^2}{\tilde{m}_{K,0}^2} - \frac{1}{2} \log \frac{\Lambda^2}{\tilde{m}_4^2} + \frac{1}{9} \log \frac{\Lambda^2}{m_{\eta,0}^2} + \frac{65}{36} \right) \right] m_{\pi,0}^4 \\
& + \frac{1}{(4\pi)^2} \left[\log \frac{m_{K,0}^2}{\tilde{m}_4^2} + \frac{4}{9} \log \frac{m_{\eta,0}^2}{m_8^2} \right] \tilde{m}_{K,0}^4 \\
& - \left[8L_4^r - 32L_6^r - \frac{1}{2(4\pi)^2} \left(\log \frac{\Lambda^2}{\tilde{m}_4^2} + \frac{4}{9} \log \frac{\Lambda^2}{m_8^2} + \frac{13}{18} \right) \right] \frac{m_{\pi,0}^4 \tilde{m}_{K,0}^2}{\mu_I^2} \\
& + \left[4L_1^r + 4L_2^r + 2L_3^r - 8L_4^r - 4L_5^r + 16L_6^r + 8L_8^r \right. \\
& \left. + \frac{1}{144(4\pi)^2} \left(36 \log \frac{\Lambda^2}{m_2^2} + 9 \log \frac{\Lambda^2}{\tilde{m}_4^2} + 4 \log \frac{\Lambda^2}{m_8^2} - \frac{47}{2} \right) \right] \frac{m_{\pi,0}^8}{\mu_I^4} \\
& + \left[8L_4^r + \frac{1}{2(4\pi)^2} \left(\log \frac{\Lambda^2}{\tilde{m}_4^2} + \frac{1}{2} \right) \right] \tilde{m}_{K,0}^2 \mu_I^2 \\
& - \frac{5m_{\pi,0}^{12}}{12(4\pi)^2 (\mu_I^4 - m_{\pi,0}^4) \mu_I^4} {}_3F_2 \left[\begin{matrix} 1, 1, \frac{7}{2} \\ 4, 5 \end{matrix} \middle| -\frac{4m_{\pi,0}^4}{\mu_I^4 - m_{\pi,0}^4} \right], \tag{6.11}
\end{aligned}$$

where the masses are

$$m_2^2 = \mu_I^2 \left[1 - \frac{m_{\pi,0}^4}{\mu_I^4} \right], \tag{6.12}$$

$$m_3^2 = \mu_I^2, \tag{6.13}$$

$$\tilde{m}_4^2 = m_4^2 + \frac{1}{4} m_{45}^2 = \tilde{m}_{K,0}^2 + \frac{1}{4} \mu_I^2 \left[1 + \frac{m_{\pi,0}^4}{\mu_I^4} \right], \tag{6.14}$$

$$m_8^2 = m_{\eta,0}^2 - \frac{1}{3} m_{\pi,0}^2 \left[1 - \frac{m_{\pi,0}^2}{\mu_I^2} \right] \tag{6.15}$$

with $\tilde{m}_{K,0}^2 = B_0 m_s = m_{K,0}^2 - \frac{1}{2} m_{\pi,0}^2$ and $m_{\eta,0}^2 = \frac{1}{3} (4m_{K,0}^2 - m_{\pi,0}^2)$. In Eq. (6.11), we have subtracted a constant such that the pressure vanishes at $\mu_I = m_\pi$.

6.2 Large m_s -mass limit

The three-flavor pressure is given in Eq. (6.11). In the large- m_s limit, one expects that the kaons and the eta decouple and one recovers the two-flavor result for the pressure (or any other thermodynamic quantity). The effect of the s -quark in this limit is simply to renormalize the couplings, a result one would obtain by integrating it out at the level of the Lagrangian to obtain a low-energy effective theory for the light mesons. Expanding the three-flavor pressure in inverse powers of $B_0 m_s$ and throwing away terms that only depend on m_s , we obtain

$$\mathcal{P}_{0+1} = \frac{1}{2} \tilde{f}^2 \mu_I^2 \left[1 - \frac{m_\pi^2}{\mu_I^2} \right] - \frac{1}{2} \tilde{f}^2 \frac{\tilde{m}_{\pi,0}^4}{m_\pi^2} \left[1 - \frac{m_\pi^2}{\mu_I^2} \right]$$

$$\begin{aligned}
& -m_{\pi,0}^4 \left[2l_1^r + 2l_2^r + l_3^r + \frac{3}{4(4\pi)^2} \left(\log \frac{\Lambda^2}{m_{\pi,0}^2} + \frac{1}{2} \right) \right] \\
& + \frac{m_{\pi,0}^8}{\mu_I^4} \left[l_1^r + l_2^r + l_3^r + \frac{1}{4(4\pi)^2} \left(\log \frac{\Lambda^2 \mu_I^2}{\mu_I^4 - m_{\pi,0}^4} - \frac{5}{6} \right) \right] \\
& + \mu_I^4 \left[l_1^r + l_2^r + \frac{1}{4(4\pi)^2} \left(\log \frac{\Lambda^4}{\mu_I^4 - m_{\pi,0}^4} + 1 \right) \right] \\
& - \frac{5m_{\pi,0}^{12}}{12(4\pi)^2(\mu_I^4 - m_{\pi,0}^4)\mu_I^4} {}_3F_2 \left[\begin{matrix} 1, 1, \frac{7}{2} \\ 4, 5 \end{matrix} \middle| -\frac{4m_{\pi,0}^4}{\mu_I^4 - m_{\pi,0}^4} \right]. \tag{6.16}
\end{aligned}$$

where we have defined

$$\tilde{B}_0 m = B_0 m \left[1 - \left(16L_4^r - 32L_6^r - \frac{2}{9(4\pi)^2} \log \frac{\Lambda^2}{\tilde{m}_{\eta,0}^2} \right) \frac{\tilde{m}_{K,0}^2}{f^2} \right], \tag{6.17}$$

$$\tilde{f}^2 = f^2 \left[1 + \left(16L_4^r + \frac{1}{(4\pi)^2} \log \frac{\Lambda^2}{\tilde{m}_{K,0}^2} \right) \frac{\tilde{m}_{K,0}^2}{f^2} \right], \tag{6.18}$$

$$l_1^r + l_2^r = 4L_1^r + 4L_2^r + 2L_3^r + \frac{1}{16(4\pi)^2} \left[\log \frac{\Lambda^2}{\tilde{m}_{K,0}^2} - 1 \right], \tag{6.19}$$

$$l_3^r = -8L_4^r - 4L_5^r + 16L_6^r + 8L_8^r + \frac{1}{36(4\pi)^2} \left[\log \frac{\Lambda^2}{\tilde{m}_{\eta,0}^2} - 1 \right], \tag{6.20}$$

with $\tilde{m}_{\pi,0}^2 = 2\tilde{B}_0 m$, $\tilde{m}_{K,0}^2 = B_0 m_s$, and $\tilde{m}_{\eta,0}^2 = \frac{4}{3}B_0 m_s$. Comparing Eqs. (6.17) and (6.18) with Eqs. (6.21) and (6.23), we see that $\tilde{B}_0 m$ and \tilde{f} contain exactly the one-loop corrections to the pion mass and the pion decay constant from the heavy mesons. Eqs. (6.19) and (6.20) are in agreement with the result obtained by Gasser and Leutwyler in Ref. [6] when comparing two and three-flavor χ PT in the large m_s -mass limit. It can be verified that the scale dependence on the left-hand and right-hand side of Eqs. (6.19) and (6.20) is the same.

6.3 Numerical results

We have expressed our result Eq. (6.11) for the pressure in terms of the bare masses $m_{\pi,0}$ and $m_{K,0}$, the bare decay constant f , the renormalized couplings $L_i^r(\Lambda)$, and the isospin chemical potential μ_I . In order to evaluate numerically thermodynamic quantities such as the pressure and the energy density consistently, we need to relate the physical masses (pole masses) to the bare ones. At leading order this was straightforward as shown in section 5.2. At next-to-leading order, this requires that we determine these relations also at next-to-leading order. We therefore need the pole masses calculated to one-loop order. Similarly, the relation between the measured pion decay constant f_π and its bare counterpart f receives radiative corrections. The relations are [6]

$$m_\pi^2 = m_{\pi,0}^2 \left[1 - \left(8L_4^r + 8L_5^r - 16L_6^r - 16L_8^r + \frac{1}{2(4\pi)^2} \log \frac{\Lambda^2}{m_{\pi,0}^2} \right) \frac{m_{\pi,0}^2}{f^2} \right]$$

Constant	Value [$\times 10^{-3}$]	Source
$L_1^r(\Lambda)$	1.0 ± 0.1	[56]
$L_2^r(\Lambda)$	1.6 ± 0.2	[56]
$L_3^r(\Lambda)$	-3.8 ± 0.3	[56]
$L_4^r(\Lambda)$	0.0 ± 0.3	[56]
$L_5^r(\Lambda)$	1.2 ± 0.1	[56]
$L_6^r(\Lambda)$	0.0 ± 0.4	[56]
$L_8^r(\Lambda)$	0.5 ± 0.2	[56]

Table 1. The renormalized coupling constants $L_i^r(\Lambda)$ of the next-to-leading order Lagrangian of three-flavor chiral perturbation theory, measured at the scale of the ρ meson, $\Lambda = m_\rho$.

$$-(L_4^r - 2L_6^r) \frac{16m_{K,0}^2}{f^2} + \frac{m_{\eta,0}^2}{6(4\pi)^2 f^2} \log \frac{\Lambda^2}{m_{\eta,0}^2} \Big], \quad (6.21)$$

$$m_K^2 = m_{K,0}^2 \left[1 - (L_4^r - 2L_6^r) \frac{8m_{\pi,0}^2}{f^2} - (2L_4^r + L_5^r - 4L_6^r - 2L_8^r) \frac{8m_{K,0}^2}{f^2} - \frac{m_{\eta,0}^2}{3(4\pi)^2 f^2} \log \frac{\Lambda^2}{m_{\eta,0}^2} \right], \quad (6.22)$$

$$f_\pi^2 = f^2 \left[1 + \left(8L_4^r + 8L_5^r + \frac{2}{(4\pi)^2} \log \frac{\Lambda^2}{m_{\pi,0}^2} \right) \frac{m_{\pi,0}^2}{f^2} + \left(16L_4^r + \frac{1}{(4\pi)^2} \log \frac{\Lambda^2}{m_{K,0}^2} \right) \frac{m_{K,0}^2}{f^2} \right]. \quad (6.23)$$

Since we are working in the isospin and with $e = 0$ limit, we only need two physical masses, in contrast to the four used in 5.2. In addition, we need the physical value of f_π and the experimental values for the renormalized couplings at a certain scale. For three flavors, the convention is that the running couplings are measured at the scale $\Lambda = m_\rho = 770$ MeV. The couplings needed are listed in Table 1, taken from Ref. [56].

In Table 2, we show the LO and NLO values for the bare parameters. At LO the bare parameters are equal to the experimental values as explained. At NLO, they are obtained by solving Eqs. (6.21)–(6.23) numerically using the physical values for m_π , m_K , f_π , and L_i^r as input. Since we will be comparing our results with recent lattice simulations [22], we use their values for the masses and the pion decay constant and not the values tabulated by the Particle Data Group [52]. The values are $m_\pi = 135.0$ MeV and $m_K = 495.0$ MeV. The simulations are carried out with two different lattices, $24^3 \times 32$ and $32^3 \times 48$ and with $f_\pi = \frac{130}{\sqrt{2}}$ and $f_\pi = \frac{136}{\sqrt{2}}$, respectively. We choose $f_\pi = \frac{133}{\sqrt{2}}$ as reasonable value. At NLO, the pion-decay constant f and the mass of kaon receive significant radiative corrections, while the pion mass is hardly affected.

In the upper left panel of Fig. 6, we show the LO (black dashed line) and NLO (red solid line) results for the pressure \mathcal{P} normalized to $\mathcal{P}_0 = f_\pi^2 m_\pi^2$ as a function of μ_I/m_π . In the

Bare parameter	LO [MeV]	NLO [MeV]	1 - LO/NLO
$m_{\pi,0}$	135.0	135.5	0.004
$m_{K,0}$	495.0	529.4	0.0649
f	$133/\sqrt{2} \approx 94.0$	80.8	-0.164

Table 2. Leading order and next-to-leading order values for the bare masses and decay constant. The values are for $\Delta m^2 = 0$ and $\Delta m_{\text{EM}}^2 = 0$. The physical values, equal to the LO values, are those used in lattice simulations [22].

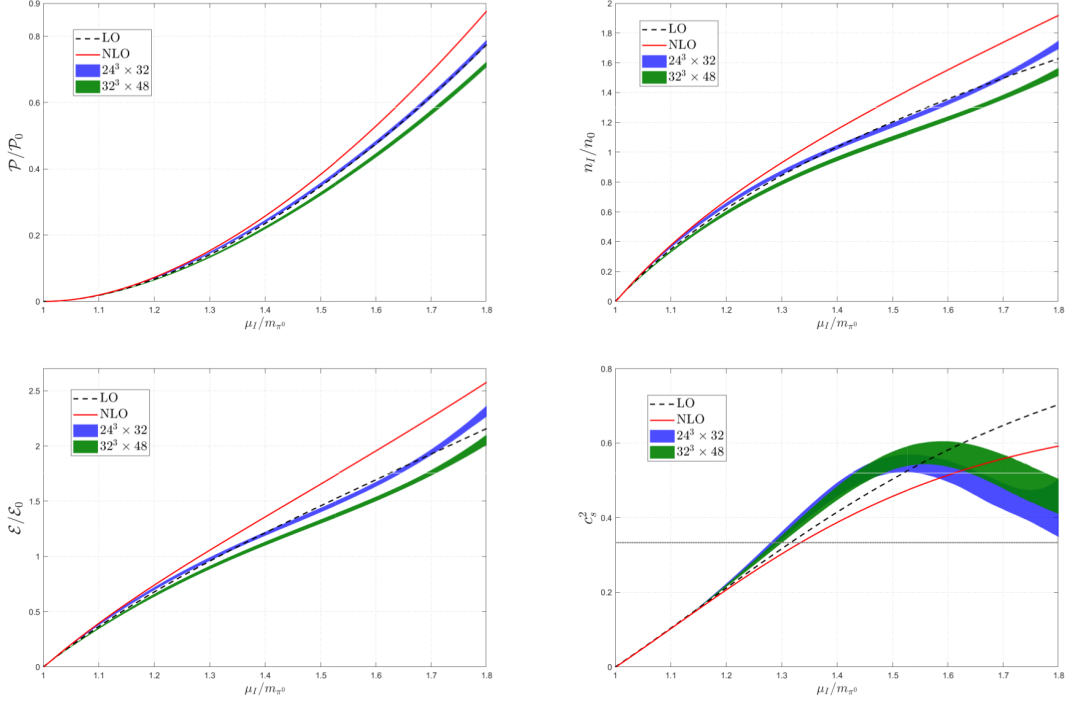


Figure 6. LO and NLO results for the speed of sound, as well as the normalized pressure, energy density, and isospin density, all functions of the normalized isospin chemical potential μ_I/m_π , where m_π is the physical pion mass at the same order as the approximation. See main text for details.

remaining panels, we show the LO and NLO results for the normalized energy density (lower left panel), normalized isospin density (upper right panel), and speed of sound squared c_s^2 (lower right panel) as functions of μ_I/m_π , with the same color coding. The energy density is normalized to $\mathcal{E}_0 = f_\pi^2 m_\pi^2$ and the isospin density to $n_0 = f_\pi^2 m_\pi$. The horizontal grey line in the lower right panel is the speed of sound in the conformal limit, $c_s^2 = \frac{1}{3}$. Note that we have normalized the isospin chemical potential to the physical pion mass determined at the same order as the approximation for the quantity in questions, the transition takes place exactly at $\mu_I/m_\pi = 1$. The correction going from LO to NLO is increasing as we increase μ_I and is rather modest for values up to $(1.3-1.4)m_\pi \approx 200$ MeV. For the sake of numerical evaluation, all NLO contributions in eq. (6.11) have been evaluated at the physical masses. That is, from line two and below, we make the substitution $m_{\pi,0} \rightarrow m_\pi$, and so on. This is

consistent to the order in χ PT we are working.

We also compare our results with two sets of lattice data. The simulations are done on a $24^3 \times 32$ (blue) and $32^3 \times 48$ lattices (green), respectively, where the bands indicate the errors. We remark in passing that in Ref. [22], the pressure and energy density are normalized to m_π^4 instead of $f_\pi^2 m_\pi^2$ and the plots therefore look somewhat different. χ PT is in good agreement in the region where it is expected to be valid. Generally, in the region where the NLO results start to deviate from the LO results, the latter is in better agreement with Monte Carlo simulations. This is in contrast to the results for the quark and pion condensates, here the NLO is in significantly better agreement with lattice results [57].

The plot of the speed of sound is perhaps particularly interesting. The prediction from χ PT is in good agreement with lattice up to values of perhaps 1.3, whereafter it fails badly: The speed of sound increases, as we increase the chemical potential, while the lattice results show a peak around 1.5, after which it decreases. χ PT is described by an EoS that in the ultrarelativistic limit is $\epsilon = p$ and therefore the speed of sound approaches the speed of light as $\mu_I \rightarrow \infty$. In contrast to this, in lattice QCD, the relevant degrees at high isospin density are fermions. The EoS of an ideal Fermi gas is $\epsilon = 3p$ and the speed of sound is $c_s = \frac{1}{\sqrt{3}}$. This is the so-called conformal limit and is shown as a horizontal dashed line in the panel. Due to asymptotic freedom it is expected that QCD approaches this limit as the density increases and the strong interaction gets weaker.

The results above are all obtained using the physical constants from the lattice simulations. If we instead use the best current measurements, as reported in the PDG [52], with

$$m_\pi = 139.57 \text{ MeV} , \quad m_K = 493.68 \text{ MeV} , \quad f_\pi = 92.07 \text{ MeV} , \quad (6.24)$$

where we chose the mass of the positively charged particles, the corresponding bare constants are also different,

$$m_{\pi,0} = 140.25 \text{ MeV} , \quad m_{K,0} = 530.55 \text{ MeV} , \quad f = 78.18 \text{ MeV} . \quad (6.25)$$

This in turn leads to slightly different thermodynamic functions. We illustrated this by plotting the normalized pressure in Fig. 7. The pressure and the chemical potential are both normalized using the lattice constants, which is why the black dashed line terminates at $\mu_I/m_\pi = 1$, while the blue line starts at a slightly higher chemical potential.

7 Chiral limit of two-flavor χ PT

In two-flavor χ PT there are three mass scales, namely the pion mass, the pion decay constant, and the isospin chemical potential.⁶ In three-flavor χ PT, we have additional mass scales, namely the kaon and eta masses, and μ_S . However, in the pion-condensed phase, the thermodynamic quantities are independent of μ_S , while in the kaon-condensed phases the relevant scales are the combinations $\mu_K = \pm \frac{1}{2} \mu_I + \mu_S$. In the chiral limit of

⁶Ignoring the small mass difference of the charged and neutral pion due to electromagnetic effects and when $\Delta m^2 \neq 0$.

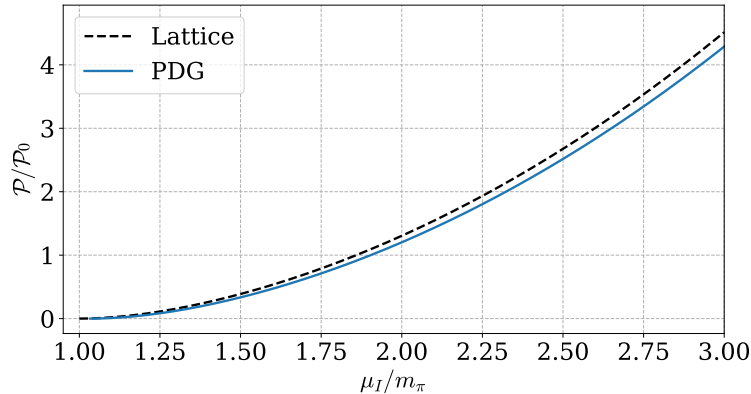


Figure 7. Comparison of results using constants from the lattice simulations and those in the PDG. Set main text for details

two-flavor QCD, we have only two mass scales and a single massless ratio, namely μ_I/f . All thermodynamic quantities can therefore be expanded in this ratio and higher-order calculations are in fact tractable. The main reason is that the propagator is diagonal and has a simple form due to the fact that $\alpha = \frac{1}{2}\pi$. It then follows that the LO pressure is $\mathcal{P}_0 = \frac{1}{2}f^2\mu_I^2$ and the pressure can be written as

$$\mathcal{P}_{0+1+2+\dots} = \frac{1}{2}f^2\mu_I^2 + a_1\mu_I^4 + a_2\frac{\mu_I^6}{f^2} + \dots \quad (7.1)$$

The pressure through $\mathcal{O}(p^4)$ in the chiral limit can be found by sending the bare pion mass $m_{\pi,0}$ to zero in Eq. (6.16). Noting that the contribution from the hypergeometric function vanishes in this limit, we obtain the coefficient a_1

$$a_1 = l_1^r(\Lambda) + l_2^r(\Lambda) + \frac{1}{2(4\pi)^2} \left[\frac{1}{2} + \log \frac{\Lambda^2}{\mu_I^2} \right]. \quad (7.2)$$

The scale dependence of the running couplings $l_1^r(\Lambda)$ and $l_2^r(\Lambda)$ in Eq. (7.2) cancels against the explicit scale dependence of $\log \frac{\Lambda^2}{\mu_I^2}$ in such a way that a_1 is independent of Λ . This remark also applies to a_2, a_3, \dots , and ensures the scale independence of the pressure order by order in the low-energy expansion.

The cubic and quartic interactions from the LO Lagrangian are

$$\mathcal{L}_2^{(3)} = \frac{\mu_I}{f} \partial_0 \phi_1 [\phi_2^2 + \phi_3^2], \quad (7.3)$$

$$\mathcal{L}_2^{(4)} = \frac{1}{6f^2} [\phi_a \phi_b (\partial_\mu \phi_a) (\partial^\mu \phi_b) - \phi_a \phi_a (\partial_\mu \phi_b) (\partial^\mu \phi_b)] + \frac{\mu_I^2}{6f^2} \phi_a \phi_a [\phi_2^2 + \phi_3^2]. \quad (7.4)$$

The NLO Lagrangian is expanded to second order in ϕ_a , which gives

$$\begin{aligned} \mathcal{L}_4^{(2)} = & -2(l_1 + l_2) \frac{\mu_I^4}{f^2} (\phi_2^2 + \phi_3^2) + 2(2l_1 + l_2) \frac{\mu_I^2}{f^2} (\partial_0 \phi_1)^2 + 2l_1 \frac{\mu_I^2}{f^2} (\partial_\mu \phi_a) (\partial^\mu \phi_a) \\ & + 2l_2 \frac{\mu_I^2}{f^2} [(\partial_\mu \phi_1) (\partial^\mu \phi_1) + (\partial_0 \phi_a)^2]. \end{aligned} \quad (7.5)$$

The order- p^6 contributions to the pressure from one-loop graphs with counterterm insertions and two-loop graphs are

$$\begin{aligned} \mathcal{P}_2^{\text{loops}} &= \frac{\mu_I^2}{6f^2} [3I_1^2(m_2^2) + 3I_1^2(m_3^2) + 2I_1(m_2^2)I_1(m_3^2)] - \frac{1}{6f^2}(m_2^2 + m_3^2)I_1(m_2^2)I_1(m_3^2) \\ &+ \frac{\mu_I^2}{f^2} [J(m_2^2) + J(m_3^2)] - (l_1 + l_2) \frac{2\mu_I^4}{f^2} [I_1(m_2^2) + I_1(m_3^2)] \\ &+ l_1 \frac{2\mu_I^2}{f^2} [m_2^2 I_1(m_2^2) + m_3^2 I_1(m_3^2)] + l_2 \frac{2\mu_I^2}{f^2} \left[\frac{m_2^2}{d+1} I_1(m_2^2) + \frac{m_3^2}{d+1} I_1(m_3^2) \right], \end{aligned} \quad (7.6)$$

where the integral $J(m^2)$ is defined in Eq. (A.10). Counterterm diagrams with a massless propagator or double-bubble diagrams with a massless propagator vanish in dimensional regularization since there is no mass scale in the corresponding integrals. Contributions from these diagrams are not included in Eq. (7.6) above. Using the fact that $m_2 = m_3 = \mu_I$ and that $J(m^2) = -I_1^2(m^2)/(d+1)$, Eq. (7.6) reduces to

$$\mathcal{P}_2^{\text{loops}} = \frac{d-1}{d+1} \frac{\mu_I^2}{f^2} I_1^2(\mu_I^2) - l_2 \frac{4d}{d+1} \frac{\mu_I^4}{f^2} I_1(\mu_I^2). \quad (7.7)$$

Note that the dependence on l_1 drops out. The contribution to the pressure from the static part of \mathcal{L}_6 is

$$\mathcal{P}_2^{\text{static}} = 2(C_{24} + C_{25} + C_{26})\mu_I^6. \quad (7.8)$$

Adding Eqs. (7.7) and (7.8), renormalizing $C = C_{24} + C_{25} + C_{26}$ according to Eq. (2.35), we obtain the NNLO contribution to the pressure. The coefficient a_2 reads

$$a_2 = 2C_r - \frac{1}{(4\pi)^2} \left[\frac{1}{2} - 3 \log \frac{\Lambda^2}{\mu_I^2} \right] l_2^r + \frac{1}{(4\pi)^4} \left[-\frac{1}{8} - \frac{1}{3} \log \frac{\Lambda^2}{\mu_I^2} + \frac{1}{2} \log^2 \frac{\Lambda^2}{\mu_I^2} \right]. \quad (7.9)$$

It can be verified that a_2 is independent of the scale Λ using the running of $l_2^r(\Lambda)$ and $C^r(\Lambda)$. Comparing the coefficients a_1 and a_2 , we note that the effective expansion parameter is $\mu_I^2/(4\pi)^2 f^2$. This suggests that the chiral limit should be a good approximation for $m_\pi \ll \mu_I \ll 4\pi f$.

8 Low-energy effective theory and phonon damping rate

In section 5, we calculated the dispersion relations for the charged and neutral mesons in the pion-condensed phase at leading order in the low-energy expansion. The Goldstone mode has a linear dispersion relation for small momentum p , which follows directly from a Taylor expansion of Eq. (5.23) around $p = 0$,

$$E_{\pi^-}(p) = \sqrt{\frac{\mu_I^4 - m_{\pi^\pm,0}^4}{\mu_I^4 + 3m_{\pi^\pm,0}^4}} p + \mathcal{O}(p^2). \quad (8.1)$$

More generally, one can ask about the low-energy dynamics and the low-energy effective theory that describes the Goldstone boson or phonon alone. Since the lightest massive

excitation is π^0 with a mass of μ_I in the broken phase, the low-energy effective theory will be valid for $p \ll \mu_I$. Son showed how to construct such a theory over two decades ago [58]. The prescription is remarkably simple: The effective theory for the GB ϕ is given in terms of the thermodynamic pressure \mathcal{P} as a function of the chemical potential and possibly other quantities such as meson masses simply by making the substitution $\mu_I \rightarrow \sqrt{\nabla_\mu \phi \nabla^\mu \phi}$, i.e.

$$\mathcal{L} = \mathcal{P}(\mu_I \rightarrow \sqrt{\nabla_\mu \phi \nabla^\mu \phi}), \quad (8.2)$$

where the covariant derivative is $\nabla_\mu \phi = \partial_\mu \phi - \delta_{\mu 0} \mu_I$. The only assumption that was made is that the dispersion relation for the phonon is linear. Eq. (8.1) is only linear for small momenta and once there are sizable corrections, the effective theory breaks down.⁷ Making the substitution in the LO pressure Eq. (5.50) with $\Delta m_{\text{EM}}^2 = 0$ and expanding the Lagrangian in powers of derivatives and rescaling the field, we obtain

$$\mathcal{L} = \frac{1}{2} \partial_0 \phi^2 - \frac{1}{2} c_s^2 (\nabla \phi)^2 - c_1 (\partial_0 \phi)^3 + c_1 \partial_0 \phi (\nabla \phi)^2 + \dots, \quad (8.3)$$

where the phonon speed c_s and the coupling c_1 are

$$c_s = \sqrt{\frac{\mu_I^4 - m_{\pi^\pm, 0}^4}{3m_{\pi^\pm, 0}^4 + \mu_I^4}}, \quad c_1 = \frac{2m_{\pi^\pm, 0}^4 \mu_I}{f} \frac{1}{(3m_{\pi^\pm, 0}^4 + \mu_I^4)^{\frac{3}{2}}}. \quad (8.4)$$

Similar results are obtained to leading order in the kaon-condensed phases upon substituting the pion mass with the appropriate kaon mass and the isospin chemical potential with the appropriate chemical potential.

We next consider loop corrections to the dispersion relation. In order to calculate the full self-energy at one loop, we need the quartic terms in the expansion Eq. (8.3), however the corresponding diagrams contribute only to its real part. The corresponding correction is simply a correction to the phonon speed which can also be calculated directly from the equation of state. In order to calculate the imaginary part and hence the damping rate, it is sufficient to consider the cubic terms. Our calculations will resemble those of Refs. [59–61], in which the leading-order phonon speed and the damping rate in the color-flavor locked phase of QCD was calculated. The expression for the relevant self-energy diagram is given by the following integral in Minkowski space

$$\Pi(P) = c_1^2 \int_Q \frac{F(P, Q)}{(q_0^2 - c_s^2 q^2)[(p_0 - q_0)^2 - c_s^2 (\mathbf{p} - \mathbf{q})^2]}, \quad (8.5)$$

where the function $F(P, Q)$ is defined as

$$F(P, Q) = 2 \left\{ 3(p_0 - q_0)p_0q_0 - (p_0 - q_0)\mathbf{p} \cdot \mathbf{q} - p_0(\mathbf{p} \cdot \mathbf{q} - q^2) - q_0(p^2 - \mathbf{p} \cdot \mathbf{q}) \right\}. \quad (8.6)$$

The integral is next rewritten using Feynman parameters, changing the variables $R = Q - Px$ and scaling $r_0, r_0 \rightarrow r_0/c_s$. The leading contribution is obtained by setting $R = 0$ in the numerator. The function $F(P, R)$ then reduces to $G(P) = F(P, 0)$, where

$$G(P) = 18x^2(1-x)^2 p_0^2 (p_0^2 - p^2)^2. \quad (8.7)$$

⁷For a color superconductor, the momenta must be much smaller than the superconducting gap Δ . For a dilute Bose gas, $p \ll (2mgn)^{\frac{1}{2}}$, where $(2mgn)^{-\frac{1}{2}}$ is the coherence length, see section 9.

After rotating to Euclidean space, we obtain

$$\Pi(P) = \frac{c_1^2}{c_s^3} \int_0^1 dx \int_R \frac{G(P)}{\left[R^2 + \frac{p_0^2 - c_s^2 p^2}{c_s^2} x(1-x) \right]^2}, \quad (8.8)$$

We next use Eq. (A.9) for the integral of momenta R . Integrating the resulting expression with respect to x and going back to Minkowski space yields

$$\Pi(P) = -\frac{3c_1^2}{5(4\pi)^2 c_s^3} p_0^2 (p_0^2 - p^2)^2 \left[\frac{1}{\epsilon} - \log \frac{p_0^2 - c_s^2 p^2}{c_s^2 \Lambda^2} + \frac{47}{30} \right]. \quad (8.9)$$

The damping rate γ is defined as

$$\gamma = -\frac{\text{Im}\Pi(P)}{E_p} \Big|_{p_0^2 = c_s^2 p^2}. \quad (8.10)$$

For $c_s^2 \ll 1$, we approximate $(p_0^2 - p^2)^2 \simeq p^4$, which yields

$$\gamma = \frac{3c_1^2}{160\pi c_s^2} p^5. \quad (8.11)$$

In the nonrelativistic limit, $c_s^2 \rightarrow \frac{\mu_{\text{NR}}}{m_{\pi^\pm,0}} = \frac{gn_I}{m_{\pi^\pm,0}} = \frac{n}{m_{\pi^\pm,0} f^2}$ and $c_1 = \frac{1}{2fm_{\pi^\pm,0}}$. This yields

$$\gamma = \frac{3p^5}{640\pi m_{\pi^\pm,0} n_I}, \quad (8.12)$$

which is the classic result by Beliaev [62] for a dilute Bose gas. In the next section, we discuss the nonrelativistic limit of χ PT and the dilute Bose gas further.

9 Dilute Bose gas and the nonrelativistic limit of χ PT

In this section, we first briefly discuss the classic textbook example of Bose condensation, namely that of a nonrelativistic dilute Bose gas. The leading correction to the energy density is derived using effective field theory methods. We then show that a pion condensate behaves nonrelativistically close to the phase transition. Finally, we recover the two-flavor results from Ref. [63] by taking the limit $m_s \rightarrow \infty$.

9.1 Dilute Bose gas

The quantum phase transition from the vacuum to the pion-condensed phase takes place at $\mu_I = m_\pi$. The (isospin) number density vanishes as $\mu_I \rightarrow m_\pi$ from above. If we consider chemical potentials very close to the pion mass, we should be able to make contact with the nonrelativistic dilute Bose. This was shown at the mean-field level in two-color QCD in Ref. [64] using the NJL model. It was shown that the diquark-diquark scattering length could be expressed in terms of the pion mass and the pion decay constant as $a_{dd} = \frac{m_\pi}{16f_\pi^2}$ and that the expressions for the pressure, baryon density, and energy density reduce to those of the homogeneous Bose gas. Here we will show similar results including loop corrections to the mean-field expressions.

The dilute Bose gas has been studied extensively for several decades beginning with the paper by Bogoliubov [65] in the 1940s. The starting point is a nonrelativistic low-energy effective field theory that describes the particles at momenta much lower than their inverse size [66]. The Lagrangian that describes the system at finite chemical potential is

$$\mathcal{L} = \psi^\dagger(i\partial_0 + \mu_{\text{NR}})\psi - \frac{1}{2m}\nabla\psi^\dagger \cdot \nabla\psi - \frac{g}{4}(\psi^\dagger\psi)^2 - \frac{g_3}{36}(\psi^\dagger\psi)^3 + \dots, \quad (9.1)$$

where the quantum field ψ^\dagger creates a particle, ψ destroys a particle, μ_{NR} is the nonrelativistic chemical potential, g , and g_3 are coupling constants. The dots indicate terms that are higher order in the number fields ψ , ψ^\dagger and their derivatives. The term $(\psi^\dagger\psi)^2$ represents two-particle scattering and the coupling g is related to the s -wave scattering length a as $g = \frac{8\pi a}{m}$. The term $(\psi^\dagger\psi)^3$ represents $3 \rightarrow 3$ scattering.

At zero temperature, the expansion parameter of the dilute Bose gas is the so-called (dimensionless) gas parameter $\sqrt{na^3}$, where n is the number density. Bogoliubov [65] obtained the mean-field results for the pressure, number density, and energy density. For example, the energy density is $\mathcal{E}(n) = \frac{2\pi an^2}{m}$. The leading corrections to Bogoliubov's results for the pressure and energy density were calculated by Lee, Huang, and Yang [67, 68] using the pseudo-potential method. Later, part of the next-to-leading order correction was calculated by Wu [69], by Hugenholtz and Pines [70], and by Sawada [71]. A complete next-to-leading result was obtained by Braaten and Nieto [72] using effective-field theory methods. The result depends not only on the scattering length a , but also on an energy-independent term in the scattering amplitude for $3 \rightarrow 3$ scattering. The result is

$$\mathcal{E}(n) = \frac{2\pi an^2}{m} \left[1 + \frac{128}{15\sqrt{\pi}}\sqrt{na^3} + \left(\frac{32\pi - 24\sqrt{3}}{3} \ln(na^3) + C \right) na^3 \right], \quad (9.2)$$

where C is a constant involving the coupling g_3 . It was already realized by Hugenholtz and Pines that physical quantities depend on other quantities than the s -wave scattering length. These effects are referred to as nonuniversal effects and are mimicked e.g. by the term $g_3(\psi^\dagger\psi)^3$ in Eq. (9.1). Similarly, the effective range r_s of the two-body potential can be included by adding the operator $h[\nabla(\psi^\dagger\psi)]^2$, where the coupling h is related to the effective range by $h = 2\pi a^2 r_s$ [73].

We now derive the first two terms in the expansion Eq. (9.2) using the effective nonrelativistic Lagrangian Eq. (9.1). The first term is the mean-field result, while the second arises from a one-loop calculation. The complex field is written as $\psi = v + \tilde{\psi}$, where $v = \langle \psi \rangle$ is its expectation value and $\tilde{\psi}$ is a fluctuating quantum field. The fluctuating field is written as $\tilde{\psi} = \frac{1}{\sqrt{2}}(\psi_1 + i\psi_2)$. To second order in the fluctuations, one finds

$$\mathcal{L}^{\text{static}} = \mu_{\text{NR}}v^2 - \frac{g}{4}v^4, \quad (9.3)$$

$$\mathcal{L}^{\text{linear}} = \frac{vX}{\sqrt{2}m}\psi_1, \quad (9.4)$$

$$\mathcal{L}^{\text{quadratic}} = \frac{1}{2}(\dot{\psi}_1\psi_2 - \psi_1\dot{\psi}_2) + \frac{1}{4m}\psi_1(\nabla^2 + X)\psi_1 + \frac{1}{4m}\psi_2(\nabla^2 + Y)\psi_2, \quad (9.5)$$

where the functions are $X = 2m(\mu_{\text{NR}} - \frac{1}{2}gv^2)$ and $Y = 2m(\mu_{\text{NR}} - \frac{3}{2}gv^2)$. The propagator matrix is

$$D(\omega, p) = \frac{i}{\omega^2 - E^2(p)} \begin{pmatrix} \frac{1}{2m}(p^2 - X) & -i\omega \\ i\omega & \frac{1}{2m}(p^2 - Y) \end{pmatrix}, \quad (9.6)$$

where the spectrum is

$$E(p) = \frac{1}{2m} \sqrt{(p^2 - X)(p^2 - Y)}. \quad (9.7)$$

The thermodynamic potential in the mean-field approximation is as usual given by minus the static part of the Lagrangian,

$$\Omega_0^{(\text{NR})}(\mu_{\text{NR}}, v) = -\mu_{\text{NR}}v^2 + \frac{g}{4}v^4. \quad (9.8)$$

The linear term vanishes at the minimum of the static Lagrangian, where $X = 0$. At the classical minimum $v_0 = \sqrt{\frac{2\mu_{\text{NR}}}{g}}$, $X = 0$, Eq. (9.8) reduces to the Bogoliubov spectrum $E_p = \frac{p}{2m} \sqrt{p^2 + 4m\mu_{\text{NR}}}$. The dispersion relation is linear for small momenta $p^2 \ll 4m\mu_{\text{NR}}$ and that of a free nonrelativistic particle for large momenta $p^2 \gg 4m\mu_{\text{NR}}$. The NLO pressure is given by thermodynamic potential evaluated at the classical minimum v_0 cf. Eqs. (3.9). This is convenient since $X = 0$. The NLO pressure is then

$$\begin{aligned} \mathcal{P}(\mu_{\text{NR}}) &= -\Omega_0(\mu_{\text{NR}}, v_0) - \Omega_1(\mu_{\text{NR}}, v_0) = \frac{\mu_{\text{NR}}^2}{g} - \frac{1}{2} \int_p E(p) = \frac{\mu_{\text{NR}}^2}{g} - \frac{1}{4m} I_{0,-1}(M^2) \\ &= \frac{\mu_{\text{NR}}^2}{g} \left[1 - \frac{16(4m)^{\frac{3}{2}} \sqrt{\mu_{\text{NR}} g^2}}{15(4\pi)^2} \right]. \end{aligned} \quad (9.9)$$

where the integrals $I_{n,m}(M^2)$ are defined in the Appendix, $M^2 = 4m\mu_{\text{NR}}$, and we have used Eq. (A.15). The number density is then given by

$$n(\mu_{\text{NR}}) = \left. \frac{d\mathcal{P}}{d\mu_{\text{NR}}} \right|_{v=v_0} = \frac{2\mu_{\text{NR}}}{g} - \frac{1}{2} I_{1,1}(M^2), \quad (9.10)$$

where we have used the recursion relation Eq. (A.5). We can invert Eq. (9.10) to obtain the chemical potential in terms of the number density. To the order we are calculating, we can make the substitution $\mu_{\text{NR}} \rightarrow \frac{1}{2}gn$ in the loop integral $I_{1,1}(M^2)$. This yields

$$\mu_{\text{NR}}(n) = \frac{1}{2}gn + \frac{1}{4}gI_{1,1}(2mgn) = \frac{4\pi an}{m} \left[1 + \frac{32}{3\sqrt{\pi}} \sqrt{na^3} \right], \quad (9.11)$$

where we have used Eq. (A.16) and $g = \frac{8\pi a}{m}$ in the last step. The energy density is then

$$\mathcal{E}(n) = -\mathcal{P} + \mu_{\text{NR}}n = \frac{1}{4}gn^2 + \frac{1}{4m} I_{0,-1}(2mgn). \quad (9.12)$$

Note that the terms involving $I_{1,1}(\mu_{\text{NR}})$ cancel in final result for the energy density. Using the result for the integral in the appendix and the expression for g in terms of the s -wave scattering length, we obtain the result of Lee, Huang and Yang [67, 68],

$$\mathcal{E}(n) = \frac{2\pi an^2}{m} \left[1 + \frac{128}{15\sqrt{\pi}} \sqrt{na^3} \right]. \quad (9.13)$$

9.2 Nonrelativistic limit of χ PT

In order to take the nonrelativistic limit of χ PT, we introduce the nonrelativistic chemical potential μ_{NR} by writing $\mu_I = m_\pi + \mu_{\text{NR}}$, where m_π is the physical pion mass. In a consistent calculation, m_π must be at the same order in the low-energy expansion as calculation of the pressure itself. Expanding the pressure Eq. (6.11) to order μ_{NR} , we obtain

$$\begin{aligned} \mathcal{P} = & 2f^2 \mu_{\text{NR}}^2 \left\{ 1 - \frac{3}{2} \frac{\delta m_\pi^2}{m_{\pi,0}^2} + [32L_1^r + 32L_2^r + 16L_3^r - 40L_4^r - 20L_5^r + 80L_6^r + 40L_7^r \right. \\ & + \left. \frac{1}{(4\pi)^2} \left(\frac{11}{4} \log \frac{\Lambda^2}{m_{\pi,0}^2} + \frac{1}{2} \log \frac{\Lambda^2}{m_{K,0}^2} + \frac{5}{36} \log \frac{\Lambda^2}{m_{\eta,0}^2} + \frac{4}{9} \right) \right] \frac{m_{\pi,0}^2}{f^2} \\ & + \left[-8L_4^r + 48L_6^r + \frac{1}{(4\pi)^2} \left(\log \frac{\Lambda^2}{m_{K,0}^2} + \frac{1}{3} \log \frac{\Lambda^2}{m_{\eta,0}^2} \right) \right] \frac{\tilde{m}_{K,0}^2}{f^2} \left. \right\} - \frac{128m_{\pi,0}^{3/2} \mu_{\text{NR}}^{5/2}}{15(4\pi)^2}, \quad (9.14) \end{aligned}$$

where the term $-\frac{3}{2} \frac{\delta m_\pi^2}{m_{\pi,0}^2}$ arises from distinguishing between m_π and $m_{\pi,0}$ in the tree-level contribution to the pressure (which is necessary for a consistent calculation). This term can be read off Eq. (6.21). Also note the last term in Eq. (9.14), which comes from the hypergeometric function. This is exactly the loop correction in Eq. (9.9). This yields

$$\begin{aligned} \mathcal{P} = & 2f^2 \mu_{\text{NR}}^2 \left\{ 1 + [32L_1^r + 32L_2^r + 16L_3^r - 16L_4^r - 8L_5^r + 32L_6^r + 16L_7^r \right. \\ & + \left. \frac{1}{(4\pi)^2} \left(\frac{7}{2} \log \frac{\Lambda^2}{m_{\pi,0}^2} + \frac{1}{2} \log \frac{\Lambda^2}{m_{K,0}^2} + \frac{1}{18} \log \frac{\Lambda^2}{m_{\eta,0}^2} + \frac{4}{9} \right) \right] \frac{m_{\pi,0}^2}{f^2} \\ & + \left[16L_4^r + \frac{1}{(4\pi)^2} \log \frac{\Lambda^2}{m_{K,0}^2} \right] \frac{\tilde{m}_{K,0}^2}{f^2} \left. \right\} - \frac{128m_{\pi,0}^{3/2} \mu_{\text{NR}}^{5/2}}{15(4\pi)^2}, \quad (9.15) \end{aligned}$$

where we have defined $\tilde{m}_{K,0} = B_0 m_s$, i.e. the bare kaon mass in the limit of large m_s . This form is particularly convenient if we are interested in this limit. Expanding Eq. (9.15) in powers of $1/m_s$, using Eqs. (6.18)–(6.20), we obtain

$$\mathcal{P} = 2\tilde{f}^2 \mu_{\text{NR}}^2 \left\{ 1 + \left[8l_1^r + 8l_2^r + 2l_3^r + \frac{1}{(4\pi)^2} \left(\frac{7}{2} \log \frac{\Lambda^2}{m_{\pi,0}^2} + \frac{1}{2} \right) \right] \frac{m_{\pi,0}^2}{f^2} \right\} - \frac{128m_{\pi,0}^{3/2} \mu_{\text{NR}}^{5/2}}{15(4\pi)^2}. \quad (9.16)$$

Using the definition Eq. (2.33) replacing the running parameters l_i^r by their counterparts \tilde{l}_i yields

$$\mathcal{P} = \frac{m_\pi}{8\pi a} \mu_{\text{NR}}^2 \left[1 - \frac{32}{15\pi} \sqrt{4m_\pi \mu_{\text{NR}} a^2} \right], \quad (9.17)$$

where we have used the two-flavor expression for the pion mass to one-loop order and the scattering length $a = -a_0^2/m_\pi$, where [6]

$$m_\pi^2 = m_{\pi,0}^2 \left[1 - \frac{m_{\pi,0}^2}{2(4\pi)^2 f^2} \bar{l}_3 \right], \quad (9.18)$$

$$a_0^2 = -\frac{m_{\pi,0}^2}{4(4\pi)f^2} \left[1 - \frac{4m_{\pi,0}^2}{3(4\pi)^2 f^2} \left(\bar{l}_1 + 2\bar{l}_2 + \frac{3}{8} \right) \right]. \quad (9.19)$$

Calculating the isospin density and the energy density, we find

$$n_I = \frac{m_\pi}{4\pi a} \mu_{\text{NR}} \left[1 - \frac{8}{3\pi} \sqrt{4m_\pi \mu_{\text{NR}} a^2} \right], \quad (9.20)$$

$$\mathcal{E}(n_I) = m_\pi n_I + \frac{2\pi a n_I^2}{m} \left[1 + \frac{128}{15\sqrt{\pi}} \sqrt{n_I a^3} \right]. \quad (9.21)$$

The first term in Eq. (9.21) is the contribution to \mathcal{E} associated with the rest mass m_π of the boson. This term is absent in Eq. (9.2) since it is automatically removed by subtracting the rest mass energy in the nonrelativistic Lagrangian Eq. (9.1). The result for the pressure is in agreement with the two-flavor result recently obtained in Ref. [63]. See also Ref. [74] for similar results.

10 Summary and Outlook

In this paper, we have discussed various aspects of Bose condensation in QCD at finite μ_I and μ_S using chiral perturbation theory, which is the low-energy effective theory describing the pseudo-Goldstone bosons, pions, kaons and eta. We have been focusing on the pion-condensed phase mainly due to the fact that in this case it is possible to compare our predictions with those of lattice QCD. However, with relatively little effort similar results for the kaon-condensed phases can be obtained. Lattice QCD and χ PT agree very well in the region where the latter is expected to be valid. Depending on taste, one can view this as a check of χ PT as an effective theory of QCD or a check of the simulations. Bose-condensation in QCD is a very rich system: in the region $\mu_I \simeq m_\pi$, we have made contact with the dilute Bose gas and the classic results by Bogoliubov, Beliaev, Lee, Yang and Huang, and others. In the ultrarelativistic limit, the Goldstone mode is exactly linear and propagates with the speed of light.

The present work can be extended in several directions. Firstly, it would be interesting to calculate the thermodynamic quantities and the phase diagram to order $\mathcal{O}(p^4)$ including electromagnetic interactions. This would require using Urech's next-to-leading order Lagrangian [34] and the evaluation of a very complicated functional determinant. In the same vein, one could calculate the meson and gauge boson masses to $\mathcal{O}(p^4)$. A more straightforward extension would be to finite temperature. In a two-flavor calculation [75], the critical line between the normal phase and the BEC phase was mapped out in the μ_I - T plane. The agreement between χ PT and lattice was only for temperatures up to approximately 30 MeV. Whether the inclusion of heavier mesons would improve the situation is an open question.

We have also noticed the disagreement between χ PT and the lattice regarding the speed of sound for large values of μ_I , which is caused by the fact that χ PT has mesonic bound states as degrees of freedom and not quarks. It would be of interest to study whether it would be possible to connect the low- μ_I region described by χ PT with the high- μ_I region using perturbative QCD including a superconducting mass gap Δ and perhaps improve the agreement with simulations in the entire range of μ_I .

Acknowledgements

Q. Yu and H. Zhou have been supported by the Natural Science Foundation of China under Grant No.12305091 and the Research Fund for the Doctoral Program of the Southwest University of Science and Technology under Contract No.23zx7122. J. O. Andersen would like to thank the Niels Bohr International Academy for kind hospitality during his stay where large part of this work was carried out. J. O. Andersen would also like to thank Prabal Adhikari and Martin Mojahed for earlier collaboration as well as Alberto Nicolis, Alessandro Podo, and Luca Santoni for useful discussions. The authors thank Bastian Brandt and Gergely Endrődi for sharing their old and updated lattice data and for discussions

A Integrals in dimensional regularization

A number of loop integrals appearing in the calculations are ultraviolet divergent. We use dimensional regularization to regulate ultraviolet divergences and introduce the following notation for the integrals in Euclidean space

$$\int_P = \int_{-\infty}^{\infty} \frac{dp_0}{2\pi} \int_p, \quad (\text{A.1})$$

where

$$\int_p = \left(\frac{e^{\gamma_E} \Lambda^2}{4\pi} \right)^\epsilon \int \frac{d^d p}{(2\pi)^d}, \quad (\text{A.2})$$

with $P = (p_0, \mathbf{p})$, $p = |\mathbf{p}|$, $d = 3 - 2\epsilon$, and Λ is the renormalization scale associated with the $\overline{\text{MS}}$ scheme. The convenience with dimensional regularization is that it automatically sets power divergences to zero and logarithmic divergences show up as poles in ϵ . We define the integrals for integers $n \geq 0$ as

$$I_n(m^2) = \int_P \frac{1}{(P^2 + m^2)^n}, \quad (\text{A.3})$$

$$I'_0(m^2) = - \int_P \log [P^2 + m^2], \quad (\text{A.4})$$

where the prime denotes differentiation with respect to the index n evaluated at $n = 0$. They satisfy the recursion relation

$$\frac{dI_n(m^2)}{dm^2} = -nI_{n+1}(m^2), \quad (\text{A.5})$$

which follows directly from the definition Eq. (A.3). The expression for $I_n(m^2)$ is

$$I_n(m^2) = e^{\gamma_E \epsilon} \frac{m^{4-2n}}{(4\pi)^2} \left(\frac{\Lambda}{m} \right)^{2\epsilon} \frac{\Gamma(n - \frac{d+1}{2})}{\Gamma(n)}. \quad (\text{A.6})$$

We need the following one-loop integrals expanded to the appropriate order in ϵ

$$I'_0(m^2) = \frac{m^4}{2(4\pi)^2} \left(\frac{\Lambda}{m}\right)^{2\epsilon} \left[\frac{1}{\epsilon} + \frac{3}{2} + \mathcal{O}(\epsilon) \right], \quad (\text{A.7})$$

$$I_1(m^2) = -\frac{m^2}{(4\pi)^2} \left(\frac{\Lambda}{m}\right)^{2\epsilon} \left[\frac{1}{\epsilon} + 1 + \frac{\pi^2 + 12}{12}\epsilon + \mathcal{O}(\epsilon^2) \right], \quad (\text{A.8})$$

$$I_2(m^2) = \frac{1}{(4\pi)^2} \left(\frac{\Lambda}{m}\right)^{2\epsilon} \left[\frac{1}{\epsilon} + \mathcal{O}(\epsilon) \right]. \quad (\text{A.9})$$

The expression for the setting sun diagram is

$$J(m^2) = \int_{PQ} \frac{p_0^2}{P^2(Q^2 + m^2)[(P + Q)^2 + m^2]}. \quad (\text{A.10})$$

More generally, for different nonzero masses, the expression for the setting sun diagram is complicated. In the present case with one massless and two equal masses, it simplifies significantly. Using Feynman parameters and averaging over angles, it can be written as a product of two $I_1(m^2)$ as

$$J(m^2) = -\frac{1}{d+1} I_1^2(m^2) = -\frac{m^4}{4(4\pi)^4} \left(\frac{\Lambda}{m}\right)^{4\epsilon} \left[\frac{1}{\epsilon^2} + \frac{5}{2\epsilon} + \frac{17}{4} + \frac{\pi^2}{6} + \mathcal{O}(\epsilon) \right]. \quad (\text{A.11})$$

In the theory of dilute Bose gases, the following integrals appear [72]

$$I_{m,n}(M^2) = \int_p \frac{p^{2m}}{p^n (p^2 + M^2)^{\frac{n}{2}}}. \quad (\text{A.12})$$

They satisfy the recursion relation

$$\frac{dI_{m,n}}{dM^2} = -\frac{1}{2} n I_{m+1,n+2}(M^2), \quad (\text{A.13})$$

which follows directly from the definition Eq. (A.12). Evaluating the integrals in dimensional regularization, we find

$$I_{m,n}(M^2) = e^{\gamma_E \epsilon} \frac{M^{3+2m-2n}}{(4\pi)^{\frac{3}{2}}} \left(\frac{\Lambda}{M}\right)^{2\epsilon} \frac{\Gamma(\frac{d-n}{2} + m) \Gamma(n - m - \frac{d}{2})}{\Gamma(\frac{n}{2}) \Gamma(\frac{d}{2})}. \quad (\text{A.14})$$

We specifically need

$$I_{0,-1}(M^2) = \frac{16}{15} \frac{M^5}{(4\pi)^2} [1 + \mathcal{O}(\epsilon)], \quad (\text{A.15})$$

$$I_{1,1}(M^2) = \frac{16M^3}{3(4\pi)^2} [1 + \mathcal{O}(\epsilon)]. \quad (\text{A.16})$$

The integrals are finite in the limit $d \rightarrow 3$ reflecting that the ultraviolet divergences are powerlike.

References

- [1] K. Rajagopal and F. Wilczek, *At the frontier of particle physics*, Vol. 3 (World Scientific, Singapore, p 2061) (2001).
- [2] M. G. Alford, A. Schmitt, K. Rajagopal, and T. Schäfer, *Rev. Mod. Phys.* **80**, 1455 (2008).
- [3] K. Fukushima and T. Hatsuda, *Rept. Prog. Phys.* **74**, 014001 (2011).
- [4] S. Weinberg, *Physica A* **96**, 327 (1979).
- [5] J. Gasser and H. Leutwyler, *Ann. Phys.* **158**, (142) (1984).
- [6] J. Gasser and H. Leutwyler, *Nucl. Phys. B* **250**, 465 (1985).
- [7] J. Bijnens, G. Colangelo and G. Ecker, *Ann. Phys.* **280**, 100 (2000).
- [8] D. T. Son and M. A. Stephanov, *Phys. Rev. Lett.* **86**, 592 (2001); *Phys. Atom. Nucl.* **64**, 834 (2001).
- [9] K. Splittorff, D. T. Son, M. A. Stephanov, *Phys. Rev. D* **64**, 016003 (2001).
- [10] J. B. Kogut and D. Toublan,
- [11] J. B. Kogut and D. K. Sinclair, *Phys. Rev. D* **66**, 014508 (2002).
- [12] J. B. Kogut and D. K. Sinclair, *Phys. Rev D* **66** 034505 (2002).
- [13] J. B. Kogut and D. K. Sinclair, *Phys. Rev D* **70** 094501 (2004).
- [14] D. K. Sinclair and J. B. Kogut, *PosLat 2006* **147** (2006).
- [15] D. K. Sinclair, J. B. Kogut, *PoS LAT 2007* **225** (2007).
- [16] B. B. Brandt and G. Endrődi, *PoS LATTICE 2016*, 039 (2016).
- [17] B. B. Brandt, G. Endrődi, and S. Schmalzbauer, *EPJ Web Conf.* **175**, 07020 (2018).
- [18] B. B. Brandt, G. Endrődi, and S. Schmalzbauer, *Phys. Rev. D* **97**, 054514 (2018).
- [19] B. B. Brandt and G. Endrődi *Phys. Rev. D* **99**, 014518 (2019)
- [20] B.B. Brandt, F. Cuteri, G. Endrődi, and S. Schmalzbauer, *Particles* **3**, 80 (2020), e-Print: 1912.07451 [hep-lat].
- [21] B. B. Brandt, Francesca Cuteri, and G. Endrődi, *PoS LATTICE2021*, 232 (2022), e-Print: 2112.11113 [hep-lat]
- [22] B. B. Brandt, Francesca Cuteri, and G. Endrődi, *JHEP* **07**, 055 (2023).
- [23] T. D. Cohen, *Phys. Rev. Lett.* **91**, 222001 (2003).
- [24] S. Carignano, A. Mammarella, and M. Mannarelli, *Phys. Rev. D* **93**, 051503 (2016).
- [25] S. Carignano, L. Lepori, A. Mammarella, M. Mannarelli, and G. Pagliaroli *Eur. Phys. J. A* **53**, 35 (2017).
- [26] T. Xia, L. He, and P. Zhuang, *Phys. Rev. D* **88**, 056013 (2013);
- [27] S. S. Avancini, A. Bandyopadhyay, D. C. Duarte, and R. L. S. Farias *Phys. Rev. D* **100**, 116002 (2019).
- [28] A. Ayala, A. Bandyopadhyay, R. L. S. Farias, L. A. Hernandez, and J. L. Hernandez, *Phys. Rev. D* **107**, 074027 (2023).
- [29] R. Chiba and T. Kojo, arXiv:2304.13920 [hep-ph].

- [30] A. Ayala, B. S. Lopes, R. L. S. Faria, L. C. Parra, e-Print: 2310.13130 [hep-ph].
- [31] M. S. Grønli and T. Brauner, *Eur. Phys. J. C* **82**, 354 (2022).
- [32] M. Mannarelli, *Particles* **2**, 411 (2019).
- [33] G. Ecker, J. Gasser, A. Pich, and E. de Rafael, *Nucl. Phys. B* **321**, 311 (1989).
- [34] R. Urech, *Nucl. Phys. B* **433**, 234 (1995).
- [35] R. Dashen, *Phys. Rev.* **183**, 1245 (1969).
- [36] U.-G. Meißner, G. Müller and S. Steininger, *Phys. Lett. B* **406**, 154 (1997).
- [37] J. Gasser, A. Rusetsky, and I. Scimemi, *Eur. Phys. J. C* **32**, 97 (2003).
- [38] M. Knecht and R. Urech, *Nucl. Phys. B* **519**, 329 (1998).
- [39] H. Leutwyler, *Annals Phys.* **235**, 165 (1994).
- [40] A. Pich, *Rept. Prog. Phys.* **58**, 563 (1995).
- [41] B. Gripaios, e-Print:1506.05039 [hep-ph]
- [42] R. Penco, e-Print: 2006.16285 [hep-th].
- [43] J. I. Kapusta, *Phys. Rev. D* **24**, 426 (1981).
- [44] H. E. Haber and H. A. Weldon *Phys. Rev. D* **25**, 502 (1982).
- [45] S. Scherer, e-Print: 0210398 [hep-ph].
- [46] J. Bijnens, G. Colangelo, and G. Ecker, *Ann. Phys.* **280**, 100 (2000).
- [47] J. Bijnens, G. Colangelo, and G. Ecker, *JHEP* **02** 020 (1999).
- [48] M. K. Johnsrud, Master thesis, NTNU 2022. Thesis and code available at <https://github.com/martkjoh/master>.
- [49] P. Adhikari, J. O. Andersen, and P. Kneshcke, *Eur. Phys. J. C* **79**, 874 (2019).
- [50] A. Nicolis and F. Piazza, *JHEP* **06**, 025 (2012).
- [51] A. Nicolis, R. Penco, F. Piazza, and R. Rattazzi, *JHEP* **06** 155 (2015).
- [52] P. A. Zyla et al. (Particle Data Group), *Prog. Theor. Exp. Phys.* 2020, 083C01 (2020).
- [53] J. Gasser and H. Leutwyler, *Phys. Rep.* **87**, 77 (1982).
- [54] A. Joyce, A. Nicolis, A. Podo, and L. Santoni, *JHEP* **09** 066 (2022).
- [55] I.S. Gradshteyn and I.M. Ryzhik, *Table of Integrals, Series, and Products*. Eighth edition (2014).
- [56] J. Bijnens and G. Ecker, *Ann. Rev. of Nuclear and Particle Science*, **64**, 149 (2014).
- [57] P. Adhikari, J. O. Andersen, and M. A. Mojahed, *Eur. Phys. J. C* **81**, 449 (2021).
- [58] D.T. Son, e-Print: 0204199 [hep-ph].
- [59] C. Manuel, A. Dobado, and F. J. Llanes-Estrada, *JHEP* **09**, 076 (2005).
- [60] C. Manuel and F. J. Llanes-Estrada, *JCAP* **08** 001 (2007).
- [61] M. A. Escobedo and C. Manuel, *Phys. Rev. A* **82**, 023614 (2010).
- [62] S. T. Beliaev, *Sov. J. Phys.* **7**, 289 (1958).
- [63] J. O. Andersen, Q. Yu, and H. Zhou, e-Print: 2306.14472 [hep-ph].

- [64] L. He, Phys. Rev. D **82**, 096003 (2010).
- [65] N. N. Bogoliubov, J. Phys. (USSR) **11**, 23 (1947).
- [66] E. Braaten and A. Nieto Phys. Rev. B **56**, 14745 (1997).
- [67] T. D. Lee and C. N. Yang, Phys. Rev. **105**, 1119 (1957).
- [68] T. D. Lee, K. Huang, and C. N. Yang, Phys. Rev. **106**, 1135 (1957).
- [69] T. T. Wu, Phys. Rev. **115**, 1390 (1959).
- [70] N. M. Hugenholtz and D. Pines, Phys. Rev. **116**, 489 (1959).
- [71] K. Sawada, Phys. Rev. **116**, 1344 (1959).
- [72] E. Braaten and A. Nieto, Eur. Phys. J. B **11**, 143 (1999).
- [73] E. Braaten, H.-W. Hammer, and S. Hermans, Phys. Rev. A **63**, 063609 (2001).
- [74] A. Nicolis, A. Podo, and L. Santoni, JHEP **09**, 200 (2023)
- [75] P. Adhikari, J. O. Andersen, and M. A. Mojahed, Eur.Phys. J. C **81**, 173 (2021).